Fermionization in one-dimensional cold atom systems

Jonathan Lindgren

June 2, 2013

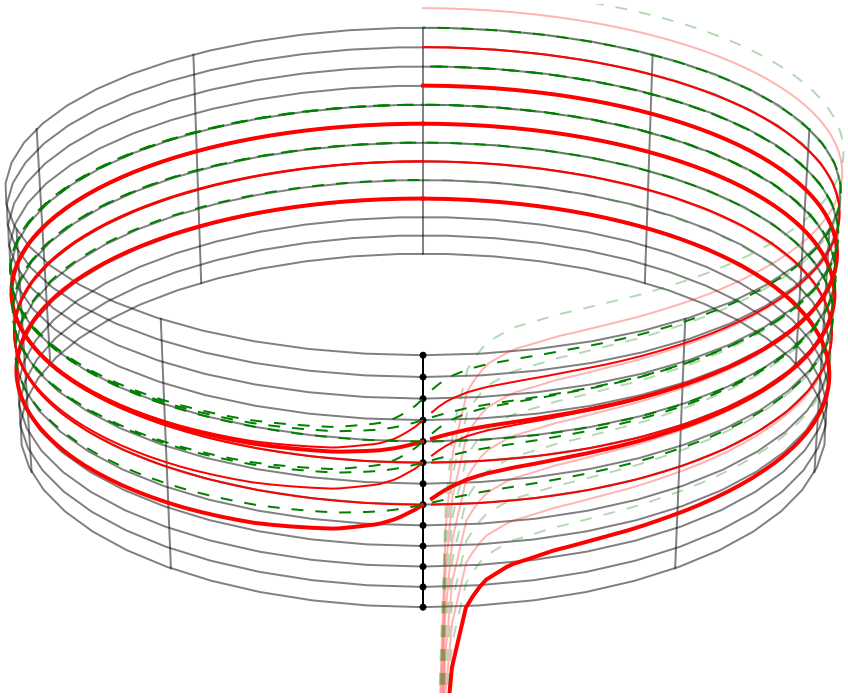

Abstract

Recent developments in experimental techniques have made it possible to use magnetic fields to tune interactions between trapped cold atoms with different spin components allowing for detailed experimental investigations of the properties of quantum mechanical few-body systems. In this thesis we investigate the properties of two-component cold atoms trapped in a harmonic oscillator potential with a zero range interaction of arbitrary strength between the different species. In the limit of infinite interaction the atoms will tend to avoid each other. This is reminiscent of the Pauli principle and we will address differences and similarities to a system of identical fermions. Exact diagonalization of the Hamiltonian in a harmonic oscillator basis is used to obtain the eigenvectors and eigenvalues of the system and we also employ numerical methods borrowed from nuclear physics to generate effective interactions using unitary transformations. This method proves to be very effective for improving the convergence and the computation time is significantly decreased even for very strongly interacting systems.

Contents

Chapter 1

Introduction

In recent years the development of new experimental tools has made it possible to cool down atoms to temperatures very close to zero kelvins. When atoms are at such low temperatures they exhibit very interesting properties since their quantum mechanical properties become significant. In particular, the atoms statistics becomes relevant. For atoms obeying Fermi-Dirac statistics the Pauli principle would become important meaning that two atoms can not be in the same quantum state. For atoms obeying Bose-Einstein statistics, atoms will instead tend to all occupy the same lowest quantum state. This phenomenon is called a Bose-Einstein condensate[11] and was discovered experimentally in 1995[1]. This was the starting point of the new field of **ultracold atoms**, which has recently been under intensive study. These systems are very interesting since they are easy to control experimentally, especially because of the so called Feshbach resonance which allows for the experimenter to basically tune the interaction strength to any desired value, see appendix A or [4]. This allows for detailed investigations of quantum mechanical phenomena and one can study fundamental properties of few-body physics with possible applications in molecular physics, condensed matter physics and nuclear physics. In this thesis we will investigate properties of a special type of system of trapped cold atoms consisting of two separated groups of atoms obeying Fermi-Dirac statistics inside each group and with an arbitrarily strong interaction between atoms from different groups.

1.1 Experimental techniques

For the quantum mechanical behaviour of atoms to become important the atoms must typically be cooled down to temperatures at the order of μK . The first step is usually laser cooling[8], where a laser is tuned to match an excitation level of the atom. Since the laser is Doppler shifted in the atoms' reference frame, it is possible to make the laser's frequency match a resonance frequency only when the atom is moving *towards* the laser and then the absorbed pho-

tons momentum will always slow down the atom instead of speeding it up. To reach even colder temperatures other methods must be employed. The atoms vibrational energy will have a distribution and thus there will be some atoms that are more energetic than others. Evaporative cooling utilizes this fact[7], where one makes the more energetic atoms escape the trapping potential and since their energy is above the average energy of the atoms the mean energy of the atoms will decrease.

1.2 Two particles with short-range interaction

The system of two distinguishable particles in a harmonic trap potential and with a short range interaction, where the interaction is modelled as a delta function (zero range) interaction $g\delta(x_1 - x_2)$, has been well studied both experimentally and theoretically[15, 3]. This system is particularly interesting since it can be solved analytically both in one, two, and three dimensions. This model is often called the Busch model after the seminal paper by Thomas Busch[3]. The energies of the even parity states are given by the solutions to the transcendental equation

$$\frac{\Gamma(-e/2 + 1/4)}{\Gamma(-e/2 + 3/4)} = -\frac{2}{g}, \tag{1.1}$$

where g is the interaction strength and e is in the units of $\hbar\omega$. Since the interaction is zero range the odd parity states are not affected and will be given by the odd parity eigenstates of the non-interaction part of the Hamiltonian. The energy spectrum as a function of g is shown in Fig. 1.1. The energy here is given in harmonic oscillator quanta $\hbar\omega$ and thus the energy spectrum without interaction is at half-integer values.

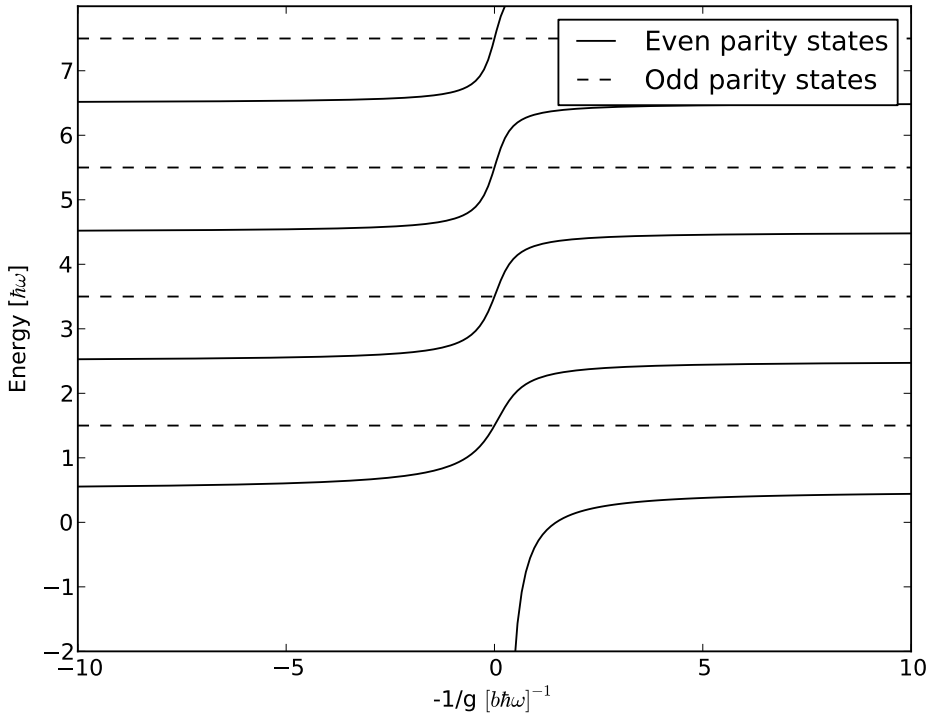

Figure 1.1: Energy spectrum of a system of two distinguishable fermions with a zero-range interaction. The odd parity states are not affected by the interaction. Only intrinsic excitations are considered, i.e. we assume that the center of mass is stationary.

Moreover, this is the intrinsic energy spectrum where the center of mass motion is considered static so thus an extra energy shift of $\frac{\hbar\omega}{2}$ is omitted. The interaction strength is given in units of $[b\hbar\omega]$ where $b = \sqrt{\frac{\hbar}{m\omega}}$ is called the oscillator length. These conventions are used throughout the thesis. At first, this was just an interesting example of an analytically solvable quantum system, but this system has now been realized in experiments by trapping cold lithium atoms using lasers and magnetic fields. The two particles are distinguishable by having different spin components. By applying an external magnetic field the two particles will be in two different hyperfine states with different magnetic moments. This gives rise to a Feshbach resonance which can be used to tune the interaction strength to any desired value, see appendix A or [4]. The particles are in a trapping potential that can be well approximated with a harmonic potential, see appendix B for more details. Furthermore, the trap is asymmetric and thus the potential has two different frequencies: $\omega_{\parallel}$ and $\omega_{\perp}$. The harmonic

potential consequently has the form

$$V(\mathbf{x}) = \frac{m\omega_{\parallel}^2}{2}x_1^2 + \frac{m\omega_{\perp}^2}{2}(x_2^2 + x_3^2). \tag{1.2}$$

The energy spacings in a quantum harmonic oscillator are given by $\hbar\omega$, thus if $\omega_\perp \gg \omega_\parallel$ the energy spacings in the perpendicular direction will be much greater and we could effectively consider the dynamics of the system as being one dimensional. In other words, the full Hilbert space is spanned by the product states $|\psi_n^{(\parallel)}\rangle \otimes |\psi_m^{(\perp)}\rangle$ where $|\psi_n^{(\parallel)}\rangle$ are eigenstates for the longitudinal part of the potential and $|\psi_m^{(\perp)}\rangle$ are eigenstates of the transverse part. We will work in the smaller space spanned by $|\psi_n^{(\parallel)}\rangle \otimes |\psi_0^{(\perp)}\rangle$. This approximation should be valid when finding the eigenstates (to the full Hamiltonian including the interaction) corresponding to the lower eigenenergies since the expansion coefficients with $m > 0$ should be negligible. However when looking at higher excited states with energies at the same order of magnitude as the energy spacing in the perpendicular direction these three-dimensional effects has to be taken into account.

When the interaction goes to positive infinity, the particles will tend to avoid each other. This is also what the Pauli principle states will happen in a system of *identical* fermions and one might ask the question how similar this system is to a system of two identical fermions. Indeed, the energy spectrum coincides with the energy spectrum of two identical fermions and this can be shown analytically[3]. This is called *fermionization*. The main topic of this thesis will be to address the differences and similarities of a fermionized few-body system and a system of an equal number of non-interacting identical fermions. It is also interesting to note in Fig. 1.1 that also when $g \to -\infty$ the energy spectrum coincides with the energy spectrum of two identical fermions (except for an additional state with energy diverging to $-\infty$) which is not as easy to explain. In Fig. 1.2 the probability density of the ground state (on the repulsive side) as a function of the two particles absolute position is plotted for several different values of g and compared to the probability density of the non-interacting state. It is evident that the probability density approaches the density of the non-interacting state. When studying systems with more particles we will study the pair correlation function which is a function of two variables and which measures the correlations between the two subsystems. The pair correlation function reduces to the total probability density in the case of two particles.

In Fig. 1.3 the relative coordinate wavefunction is shown for different values of g for the ground state on the repulsive side. Here we note that the wavefunction does not approach the non-interacting state as $g \to \infty$. Indeed, the non-interacting state is the totally antisymmetric state for two particles while the ground state, being the ground state of two distinguishable particles, is a bosonic (symmetric) state. However, in Fig. 1.4 the absolute square of the wavefunction is shown and indeed this one approaches the probability density for the non-interacting state. This is not unexpected since it is the probability

density that is directly observable, not the wavefunction itself.

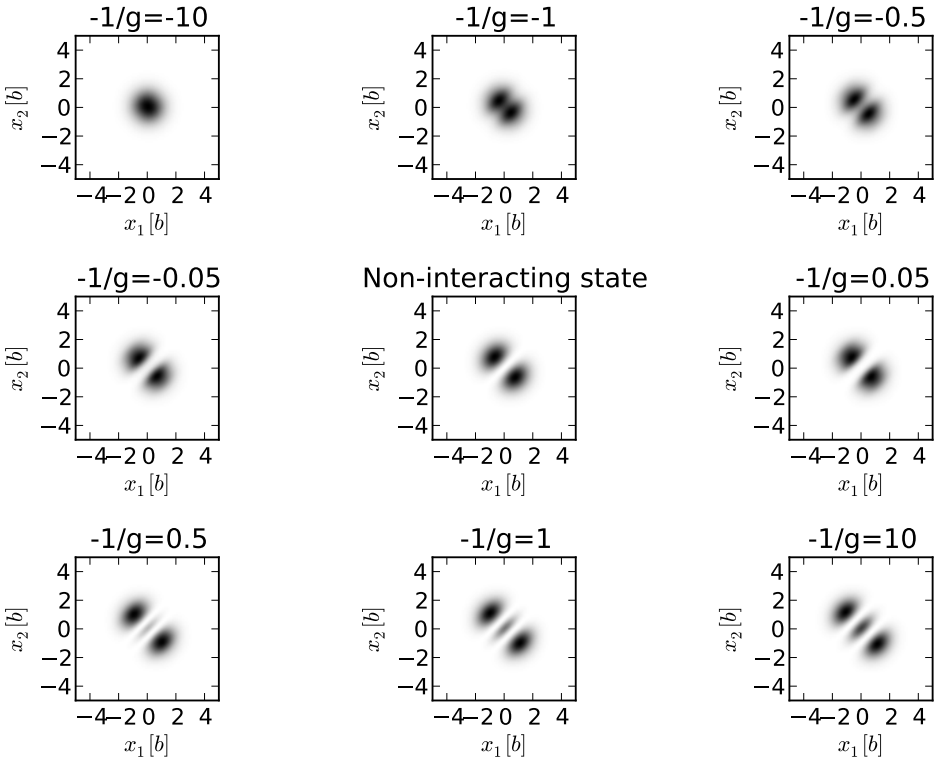

Figure 1.2: Total probability density of the two-particle system in absolute coordinates for the (repulsive side's) ground state as it changes through the spectrum as a function of g. At $g \to \pm\infty$ it coincides with the probability density fo the lowest non-interacting state which is shown in the middle.

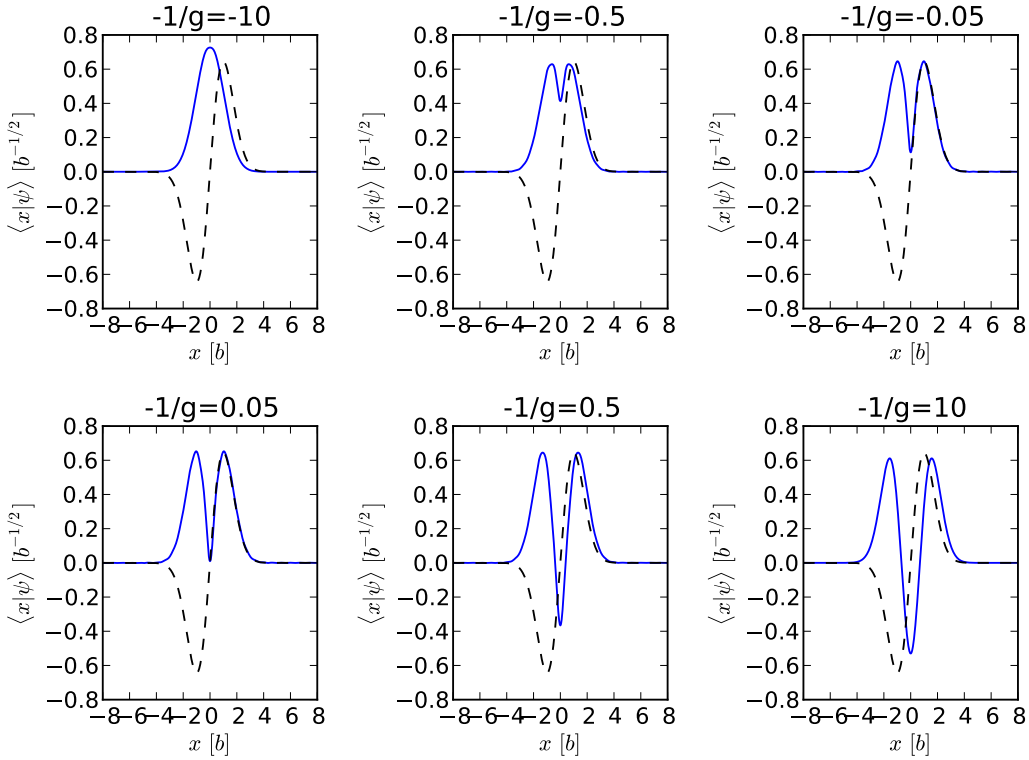

Figure 1.3: Relative wavefunction for the two-particle system for the (repulsive side) ground state as it changes through the spectrum as a function of g. The dashed lines are for the first non-interacting state.

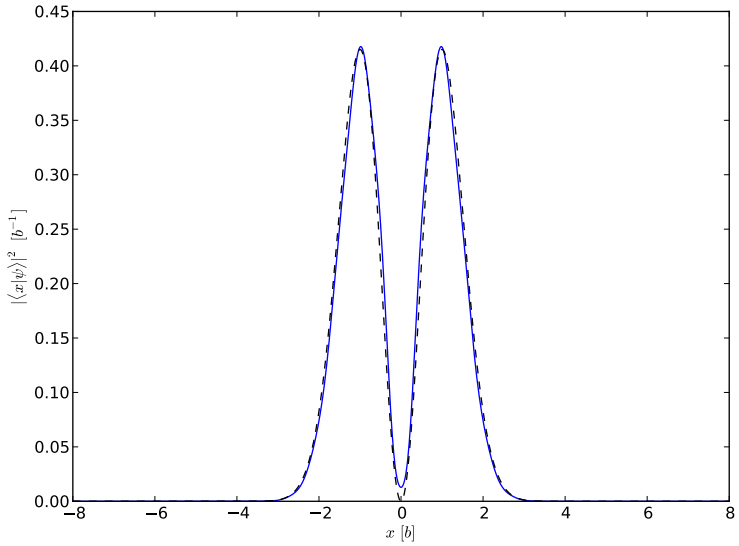

Figure 1.4: Relative probability density for the two-particle system for the ground state at strong repulsive interaction ($-1/g = 0.05$). The dashed lines is for the first non-interacting state.

In this thesis we will consider a generalization of this two-particle system which consists of two separate groups of fermions. In each group the fermions are indistinguishable but particles from different groups are considered distinguishable. This system is realized in experiments by using cold atoms in more or less the same settings as the two-particle system. Since the experiments are carried out with particles which are distinguished by having different spin components we will denote the number of particles in each subsystem $n_\uparrow$ and $n_\downarrow$, respectively. The total number of particles will thus be $n_\mathrm{t} = n_\uparrow + n_\downarrow$. Moreover, there is an interaction between particles from different groups but no interaction between the indistinguishable particles. The interaction arises though a Feshbach resonance in the same way as the interaction in the two-particle system. The applied magnetic field will put particles with different spin components in different hyperfine states. Only particles in different hyperfine states will interact. The interaction will be the same short range interaction as in the analytically solvable two-particle case. There is also the same external harmonic trapping potential for all particles. Thus the Busch model is the special case $n_\uparrow = n_\downarrow = 1$. We will focus on the case where $n_\uparrow > n_\downarrow = 1$ since this is the configuration most relevant for experiments. A major difference to the two-particle case is that this system can not be solved analytically except in the extreme cases where $g \in \{\infty, -\infty, 0\}$.

1.3 Units and conventions

We will work in harmonic oscillator units where energies are given in units of $\hbar\omega$ and lengths are given in units of the oscillator length $b = \sqrt{\frac{\hbar}{m\omega}}$. Momentum is then given in units of $\frac{\hbar}{b} = \sqrt{\hbar m\omega}$. In these units, the Hamiltonian for a simple harmonic oscillator looks like

$$H = \frac{p^2}{2} + \frac{x^2}{2}. \tag{1.3}$$

The energy spectrum would be

$$\frac{1}{2}, \frac{3}{2}, \frac{5}{2}, \dots \tag{1.4}$$

and the creation and annihilation operators are simply

$$\begin{aligned} a &= \frac{x + ip}{\sqrt{2}} \\ a^\dagger &= \frac{x - ip}{\sqrt{2}}. \end{aligned} \tag{1.5}$$

The eigenfunctions corresponding to the energy $\hbar\omega(k + \frac{1}{2})$ of a harmonic oscillator will always be denoted by $\phi_k(x)$. For n non-interacting particles in a harmonic oscillator potential the energy spectrum would be

$$E(k_1, \dots, k_n) = \frac{n}{2} + k_1 + \dots + k_n. \tag{1.6}$$

for all possible $k_j \geq 0$. However, we will consider only the intrinsic spectrum where the center of mass motion has been factored out, and thus the ground energy will instead be $E_0 = \frac{n-1}{2}$.

We will let $n_\uparrow$ and $n_\downarrow$ denote the number of particles of the respective spin species and $n_t = n_\downarrow + n_\uparrow$.

Chapter 2

Theoretical Background

In this chapter the theory of the system will be discussed. We will start with the two-particle system and work out the eigenstates and energies analytically then continue by describing the general case.

2.1 Two particle case

In this section we will find the analytic formulas of the energies and eigenvectors for the two-particle case. These will turn out to be crucial when computing the effective interaction for systems with more than two particles, see section 2.8.

2.1.1 Point-interaction matrix elements

To model a short-range interaction we will use a delta function interaction which essentially is an interaction with zero range. In the subspace of two particles it is defined by its matrix elements in relative coordinate space as

$$\langle x|V|x'\rangle = g\delta(x-x')\delta(x), \tag{2.1}$$

where $x = x_1 - x_2$ and $x' = x_1' - x_2'$ are the relative coordinates of the two particles for the two different states in the matrix element. We will compute this interaction in the harmonic oscillator basis $|n\rangle$, which are eigenstates of the Hamiltonian

$$H_\omega = \frac{p^2}{2\mu} + \mu\omega^2\frac{x^2}{2} \tag{2.2}$$

We thus have

$$\begin{aligned}\langle n|V|n'\rangle &= \int \mathrm{d}x \int \mathrm{d}x' \langle n|x\rangle\langle x|V|x'\rangle\langle x'|n'\rangle \\ &= g\int \mathrm{d}x \int \mathrm{d}x' \langle n|x\rangle\delta(x-x')\delta(x)\langle x'|n'\rangle \\ &= g\langle n|0\rangle\langle 0|n'\rangle = g\psi_n(0)\psi_{n'}(0)\end{aligned} \tag{2.3}$$

where $\psi_n(x) = \psi_n(x)^*$ are the eigenfunctions of the Hamiltonian (2.2) in position space[13]

$$\phi_n(x) = \frac{1}{\sqrt{2^n n!}} \left(\frac{\mu\omega}{\pi\hbar}\right)^{\frac{1}{4}} \exp(-\frac{\mu\omega x^2}{2\hbar}) H_n(\sqrt{\frac{\mu\omega}{\hbar}} x) \tag{2.4}$$

where H_n are the Hermite polynomials. These can be obtained via their standard generating function which is

$$\exp(2xt - t^2) = \sum_{n=0}^{\infty} H_n(x) \frac{t^n}{n!}. \tag{2.5}$$

We are only interested in their value at the origin, so letting $x = 0$ we obtain

$$\sum_{n=0}^{\infty} H_n(0) \frac{t^n}{n!} = \sum_{k=0}^{\infty} \frac{t^{2k}}{k!} (-1)^k \tag{2.6}$$

From which we see that $H_{2k+1}(0) = 0$ and $H_{2k}(0) = (-1)^k \frac{(2k)!}{k!}$. For the matrix elements we thus obtain

$$\langle n|V|n'\rangle = 0 \tag{2.7}$$

if n or n' are odd, and

$$\langle 2m|V|2m'\rangle = \frac{g}{\sqrt{\frac{\hbar}{\omega\mu}}} (-1)^{m+m'} 2^{-m-m'} \frac{1}{m!m'!} \sqrt{\frac{(2m!)(2m'!)}{\pi}}. \tag{2.8}$$

Here we can identify $\sqrt{\frac{\hbar}{\omega\mu}}$ as the natural unit in "oscillator coordinates" for the interaction strength g.

2.1.2 Energy spectrum

We recall from section 2.1.1 that the delta function interaction $V(x) = \hbar\omega g\delta(x)$ in the harmonic oscillator basis is

$$\langle n|V|m\rangle = g\hbar\omega\phi_n(0)\phi_m(0) \tag{2.9}$$

where ϕ_n is the eigenfunction of the harmonic oscillator. Let $|\psi\rangle$ be an eigenfunction to the total Hamiltonian and E be its corresponding eigenvalue and denote $c_n = \langle n|\psi\rangle$. Then we get, assuming that $E \neq E_n$ for all n where E_n is the eigenvalue to the harmonic oscillator eigenstate $|n\rangle$

$$\begin{aligned}(H_{osc} + V)|\psi\rangle = E|\psi\rangle \Rightarrow & E_n\langle n|\psi\rangle + \sum_m \langle n|V|m\rangle\langle m|\psi\rangle = E\langle n|\psi\rangle \\ \Rightarrow & c_n = \hbar\omega g\phi_n(0) \sum_m \frac{\phi_m(0)c_m}{E - E_n} \equiv \hbar\omega g\phi_n(0) \frac{A}{E - E_n},\end{aligned} \tag{2.10}$$

where the non-zero constant A is defined as $A \equiv \sum_m \phi_n(0)c_n$. Now we multiply both sides by $\phi_n(0)$ and sum over n and then cancel A from both sides to get

$$1 = \hbar\omega g \sum_m \frac{\phi_m(0)^2}{E - E_m} = \frac{g}{2} \sum_m \frac{\phi_m(0)^2}{(e/2 - 1/4) - m/2}, \tag{2.11}$$

where $E = \hbar\omega e$ and $E_m = \hbar\omega(m + 1/2)$. Now we use

$$\frac{1}{z} = \int_0^\infty \frac{dy}{(1+y)^2} \left(\frac{y}{1+y}\right)^{z-1}, \tag{2.12}$$

with $z = -(e/2 - 1/4) + m/2$, to get

$$1 = -\frac{g}{2} \int_0^\infty \frac{dy}{(1+y)^2} \left(\frac{y}{1+y}\right)^{-e/2-3/4} \sum_m \phi_m(0)^2 \left(\frac{y}{1+y}\right)^{\frac{m}{2}}. \tag{2.13}$$

We also have the following generating function for the squares of the Hermite polynomials[12]:

$$\sum_n \frac{H_n(x)^2}{2^n n!} z^n = (1-z^2)^{-1/2} \exp[2x^2 z/(1+z)] \Rightarrow \sum_n \frac{H_n(0)^2}{2^n n!} z^n = (1-z^2)^{-1/2}. \tag{2.14}$$

Together with the explicit formula for the eigenfunctions evaluated at zero

$$\phi_n(0) = \sqrt{\frac{1}{2^n n!}} \left(\frac{m\omega}{\pi\hbar}\right)^{1/4} H_n(0), \tag{2.15}$$

we obtain

$$\begin{aligned} 1 =& -G \int_0^\infty \frac{dy}{(1+y)^2} \left(\frac{y}{1+y}\right)^{-e/2-3/4} (1 - \left(\frac{y}{1+y}\right))^{-1/2} \\ =& -G \int_0^\infty \frac{dy}{(1+y)^2} \left(\frac{y}{1+y}\right)^{-e/2-3/4} \left(\frac{1}{1+y}\right)^{-1/2} \\ =& -G \int_0^\infty \frac{dy}{(1+y)^{3/4-e/2}} y^{-e/2-3/4}. \end{aligned} \tag{2.16}$$

where $G = \frac{g}{2}\left(\frac{m\omega}{\pi\hbar}\right)^{1/2}$. Now we use the relation ($z = 0$,$a = -e/2 + 1/4$,$b = 1/2$) for the confluent hypergeometric function[10]

$$\Gamma(a)U(a,b,z) = \int e^{-zt} t^{a-1} (1+t)^{b-a-1}, \tag{2.17}$$

to get

$$-G\Gamma(-e/2 + 1/4)U(-e/2 + 1/4, 1/2, 0) = 1. \tag{2.18}$$

Using the identity

$$U(a,b,0) = \frac{\pi}{\sin \pi b} \left(\frac{1}{\Gamma(1+a-b)\Gamma(b)}\right), \tag{2.19}$$

we finally obtain (remembering that $\Gamma(1/2) = \sqrt{\pi}$)

$$\begin{aligned} &- G\frac{\Gamma(-e/2+1/4)}{\Gamma(-e/2+3/4)}\sqrt{\pi} = 1 \\ \Rightarrow &\frac{\Gamma(-e/2+1/4)}{\Gamma(-e/2+3/4)} = -\frac{2}{\frac{g}{\left(\frac{\hbar}{m\omega}\right)^{1/2}}} \\ \Rightarrow &\frac{\Gamma(-e/2+1/4)}{\Gamma(-e/2+3/4)} = -\frac{2}{g'}, \end{aligned} \tag{2.20}$$

which is the Busch formula (g' is the dimensionless coupling constant).
If $E = E_n$ we can see that n has to be odd and that $|\psi\rangle = |n\rangle$, which follows from the fact that the interaction commutes with the parity operator and that the matrix elements for the interaction is zero for odd n (odd parity) and thus the odd parity states and energy levels remain unchanged by the interaction.

2.1.3 Eigenstates

We will now compute the expansion coefficients $\langle n|\psi\rangle = c_n$ of the wavefunction. To do this we return to the expression (2.10).

$$c_n = \hbar\omega g A\phi_n(0)\frac{1}{E - E_n} \tag{2.21}$$

To find A we need to use the normalization condition $\sum c_n^2 = 1$, and by using exactly the same expression for the sum before we get

$$\begin{aligned} 1 &= \frac{A^2g^2}{4}\sum_m \frac{\phi_m(0)^2}{((e/2-1/4)-m/2)^2} = -A^2 g\frac{d}{de}\left[\frac{g}{2}\sum\frac{\phi_m(0)^2}{(e/2-1/4)-m/2}\right] \\ &= A^2 gG\frac{d}{de}\left[\frac{\Gamma(-e/2+1/4)}{\Gamma(-e/2+3/4)}\sqrt{\pi}\right] \\ &= A^2\frac{g^2}{2\left(\frac{\hbar}{m\omega}\right)^{1/2}}\frac{d}{de}\left[\frac{\Gamma(-e/2+1/4)}{\Gamma(-e/2+3/4)}\right] \\ &= A^2 gg'/2\frac{d}{de}\left[\frac{\Gamma(-e/2+1/4)}{\Gamma(-e/2+3/4)}\right] \end{aligned} \tag{2.22}$$

The derivative can be expressed in the digamma function $\psi = \Gamma'/\Gamma$ by using the quotient rule and the energy constraint (2.20)

$$\begin{aligned}\frac{d}{de}(\Gamma/\Gamma) &= \frac{-1}{2}\left(\frac{\Gamma'(-e/2+1/4)\Gamma(-e/2+3/4)-\Gamma'(-e/2+3/4)\Gamma(-e/2+1/4)}{\Gamma(-e/2+3/4)^2}\right)\\ &= \frac{-1}{2}\left(\psi(-e/2+1/4)(-\frac{2}{g'})-\psi(-e/2+3/4)(-\frac{2}{g'})\right)\\ &= \frac{1}{g'}\left(\psi(-e/2+1/4)-\psi(-e/2+3/4)\right).\end{aligned} \tag{2.23}$$

So the expression for the constant A (chosen real and positive) is

$$A = \sqrt{\frac{2}{g(\psi(-e/2+1/4)-\psi(-e/2+3/4))}}, \tag{2.24}$$

and the expansion coefficients for the eigenstate in the harmonic oscillator basis is

$$c_n = \sqrt{\frac{2g}{\psi(-e/2+1/4)-\psi(-e/2+3/4)}}\phi_n(0)\frac{1}{e-n-1/2}. \tag{2.25}$$

2.1.4 Odd parity states

The odd parity states are not affected by the interaction, thus these are just harmonic oscillator eigenstates for the non-interacting part of the Hamiltonian. This will be shown later for the general case in Section 2.6. Odd parity means odd harmonic oscillator quantum number and gives a totally antisymmetric state. Thus the energy spectrum for the odd parity states are

$$\hbar\omega\frac{3}{2}, \hbar\omega\frac{7}{2}, \hbar\omega\frac{11}{2}, \ldots \tag{2.26}$$

and the corresponding eigenvectors are

$$\langle n|\psi_m\rangle = \delta_{n,2m+1} \tag{2.27}$$

where m is the m:th odd parity state starting at zero.

2.2 General case

Now we will go on and study the general case. The Hamiltonian of the system is

$$\begin{aligned}H =& \sum_{k=0}^{n_\uparrow}\left(\frac{p_{\uparrow,k}^2}{2m}+\frac{m\omega^2}{2}x_{\uparrow,k}^2\right)+\sum_{k=0}^{n_\downarrow}\left(\frac{p_{\downarrow,k}^2}{2m}+\frac{m\omega^2}{2}x_{\downarrow,k}^2\right)+\sum_{k_\uparrow=0}^{n_\uparrow}\sum_{k_\downarrow=0}^{n_\downarrow}V_{k_\uparrow,k_\downarrow}\\ =& H_0+V.\end{aligned} \tag{2.28}$$

where $n_\uparrow$ and $n_\downarrow$ are the number of particles in the two subsystems, $V_{k_\uparrow,k_\downarrow}$ are interaction terms and H_0 is the non-interacting part of the Hamiltonian. The interaction terms are only between particles from different subsystems and $p_{j,k}$ and $x_{j,k}$ are the momentum and coordinate operators for particle k in subsystem $j \in \{\uparrow,\downarrow\}$, so $p_{\uparrow,k} = p_k \otimes I$ and $p_{\downarrow,k} = I \otimes p_k$.

2.2.1 Description of the many-body basis states

The many body basis states will be tensor products of the many body states from each spin species. We will henceforth call the states for the full system many-body states and the states from one subsystem few-body states.

For n distinguishable particles it is convenient to use a basis state which is a product of n single-particle states.

$$|\psi_\alpha\rangle = |m_1\rangle \otimes \ldots \otimes |m_n\rangle. \tag{2.29}$$

As single-particle states we will use harmonic oscillator basis states with angular frequency chosen conveniently to be the angular frequency of the external harmonic trap. The state $|m_k\rangle$ here thus represents a harmonic oscillator eigenstate corresponding to eigenvalue m_k with respect to the number operator $a_k^\dagger a_k$. This is very convenient since it will make these few-body states eigenstates H_0, the non-interacting part of the Hamiltonian.

However, in each subsystem, the particles are identical fermions and it is necessary to antisymmetrize the few-body states. Thus we write

$$|(m_1, m_2, \ldots, m_n)\rangle = \frac{1}{\sqrt{n!}} \sum_{\sigma \in \mathrm{Sym}(n)} \mathrm{sign}[\sigma] |m_{\sigma(1)}\rangle \otimes \ldots \otimes |m_{\sigma(n)}\rangle, \tag{2.30}$$

where we by convention choose $m_1 > \ldots > m_n$ and $\mathrm{Sym}(n)$ is the group of permutations of n elements. These states also form an orthonormal set and we will use this notation with regular brackets to denote antisymmetrized states.

The full Hilbert space for the two systems is now just the tensor product of the two subsystems Hilbert spaces, thus we can write a complete basis for the full system as

$$|(m_1, m_2, \ldots, m_{n_\uparrow})\rangle \otimes |(k_1, k_2, \ldots, k_{n_\downarrow})\rangle. \tag{2.31}$$

We will hencefourth omit the symbol $\otimes$ for the tensor product.

2.2.2 Matrix elements of the Hamiltonian

To represent the Hamiltonian as a matrix we will evaluate its matrix elements in the many-body basis. The different parts of the Hamiltonian are either only one-particle operators (the kinetic energy operators and the harmonic trap operators) or operators coupling two particles (the interaction operators). Thus

many matrix elements will vanish since the operators will be diagonal in many of the single particle indices and we will be dealing with a sparse matrix. We can write the Hamiltonian as

$$H = H_0 + V \tag{2.32}$$

where H_0 includes the kinetic energy and the trap potential. By construction, our many-body basis states are eigenstates of H_0 and thus the contribution from this part is trivial. The interaction part is more difficult. The interaction is a sum of all possible interactions between a particle in one subsystem and one particle in the other subsystem.

$$V = \sum_{k_\uparrow=0}^{n_\uparrow} \sum_{k_\downarrow=0}^{n_\downarrow} V_{k_\uparrow,k_\downarrow}, \tag{2.33}$$

where $V_{i,j}$ is the interaction operator between particle number i in subsystem one and particle j in subsystem two. Of course, our particles are identical so we can't really separate an interaction between two particles from an interaction between two other particles, but our antisymmetric states are constructed from basis states of separable particles and thus it is convenient to first think of the interaction operators as being between specific particles in the two subsystems. However, all terms in the sum give equal values so the sum just gives a factor $n_1 \cdot n_2$. The matrix element from the interaction part thus is

$$\begin{aligned} M =& n_1 n_2 \langle (m_1, m_2, \ldots, m_{n_1})| \langle (k_1, k_2, \ldots, k_{n_2})| V_{00} \\ & |(m'_1, m'_2, \ldots, m'_{n_1})\rangle |(k'_1, k'_2, \ldots, k'_{n_2})\rangle \end{aligned} \tag{2.34}$$

where V_{00} now couples the quantum number indices in the first argument of the bras and kets for the subsystems. The resulting matrix element in the two-body subspace will be denoted $\langle a, b|V|c, d\rangle \equiv V_{abcd}$. Now we write out the antisymmetrization explicitly and use that the interaction operator is diagonal in all other $n_1 + n_2 - 2$ indices to get

$$\begin{aligned} M =& \frac{1}{(n_1-1)!(n_2-1)!} \sum_{\sigma,\sigma' \in \mathrm{Sym}(n_1), \tau, \tau' \in \mathrm{Sym}(n_2)} \mathrm{sign}[\sigma\tau\sigma'\tau'] V_{m_{\sigma(1)} k_{\tau(1)} m'_{\sigma'(1)} k'_{\tau'(1)}} \\ & \delta_{m_{\sigma(2)}, m'_{\sigma'(2)}} \ldots \delta_{m_{\sigma(n_1)}, m'_{\sigma'(n_1)}} \delta_{k_{\tau(2)}, k'_{\tau'(2)}} \ldots \delta_{k_{\tau(n_2)}, k'_{\tau'(n_2)}} \end{aligned} \tag{2.35}$$

The delta functions restrict the possible many-body states that will give a non-zero matrix element on the interaction part. Only states that differ with at most one single particle quantum number in each subsystem will work. Furthermore, the permutations will be restricted since they must put the quantum numbers at the right place for the delta functions not to vanish. If the two states differ with one single particle quantum number the permutations need to put the different quantum numbers at the first position i.e $m_{\sigma(1)}$, $m'_{\sigma'(1)}$, $k_{\tau(1)}$ and $k'_{\tau'(1)}$ must be the different quantum numbers. We also need the permutations

to make $m_{\sigma(i)} = m'_{\sigma'(i)}$ and $m_{\tau(i)} = m'_{\tau'(i)}$ for $i \geq 2$ for each delta function not to vanish. Moreover, given a permutation σ, we can always fix σ' such that the delta functions don't vanish (given that the criteria for $\sigma(1)$ and $\sigma'(1)$ are satisfied. Thus we can only specify one of the permutations and this will give a factor of $(n_1 - 1)!(n_2 - 1)!$ to exactly cancel the prefactor and we get

$$M = \text{sign}[\sigma\tau\sigma'\tau']V_{m_{\sigma(1)}k_{\tau(1)}m'_{\sigma'(1)}k'_{\tau'(1)}} \tag{2.36}$$

where the sign here is specific for the two many-body states and are not depending on the specific permutations used as long as they satisfy the above mentioned criteria. For states that differ with more than one quantum number in any of the subsystems the matrix element vanishes completely. We also need to include the diagonal matrix elements where either one or both of the few-body states are equal. Efficient algorithms for locating states that differ with at most one quantum number will be discussed in the implementation section.

2.3 Harmonic oscillator interaction

An important test case is the Harmonic oscillator interaction which is on the form

$$V = \frac{m\omega^2}{2}x^2 \tag{2.37}$$

where x is the relative coordinate between two particles and ω is the angular frequency of the oscillations. This interaction is important since it can be solved analytically for all particle systems and can thus provide a very good way to test the numerical procedure. Note, however, that it is very different from the delta function interaction (the interaction increases with increasing distance). It is also very suitable since the basis states are harmonic oscillator eigenstates which makes the numerics converge very quickly. This has the advantage that we can test the correctness of the code and algorithms used although we can't test the convergence for other interactions.

Consider a Hamiltonian for n particles with some harmonic interaction between some of the particles

$$H = \sum_{i=0}^{n}(\frac{p_i^2}{2m} + \frac{m\omega^2 x_i^2}{2}) + \sum_{i,j}\frac{m\omega_{i,j}^2}{2}(x_i - x_j)^2. \tag{2.38}$$

In our case the interaction is only between different species so $\omega_{i,j} = \omega'$ if i and j are indices from different spin species and zero otherwise. The solution for any general kind of harmonic interaction can be found by expanding the interaction squares and writing it as

$$V = X^T M X \tag{2.39}$$

where X includes all coordinates of all particles and M is a symmetric matrix. We can diagonalize M as $M = U^T DU$ for an orthogonal matrix U, so we can invent new coordinates $J = UX$ and $T = UP$. Since the non-interaction part can be written on the same form, but with the identity matrix sandwiched between X and P these terms will remain diagonal after the coordinate transformation and we get

$$H = \sum_i (\frac{t_i^2}{2m} + \frac{m\omega^2 j_i^2}{2}) + \frac{m\omega'^2}{2} \sum \lambda_i j_i^2 = \sum_i (\frac{t_i^2}{2m} + \frac{m(\omega^2 j_i^2 + \omega'^2 \lambda_i)}{2}) \quad (2.40)$$

We have now arrived at a Hamiltonian consisting of n independent harmonic oscillators, with energy levels

$$E = \sum_i E_i^{m_i}$$

, where

$$E_i^{m_i} = \hbar\sqrt{\omega^2 + \lambda_i \omega'^2}(m_i + \frac{1}{2})$$

.

For identical particles one then also needs to constraint the energy spectrum to satisfy the required statistics.

2.4 Dealing with center of mass excitations

The motion of the center of mass of the system of particles is not very interesting. One is mostly interested in the relative excitations of the system. In Jacobi coordinates this is automatically taken care of where all the degrees of freedom are relative coordinates, but since we are working with single particle coordinates this is a bit more tricky. One method to deal with this problems is to shift the Hamiltonian by the center of mass number operator

$$H \to H + \lambda N - \frac{1}{2}\hbar\omega \quad (2.41)$$

where $N = A^\dagger A$ which is the number operator for the center of mass excitations. Thus all the interesting states which have eigenvalues zero with respect to N are unaffected. By choosing λ adequately we can then shift the states with center of mass excitations away from the part of the spectrum we are interested in. This procedure works since the eigenstates will be product states of a relative motion wavefunction and a center of mass wavefunction, ie $|\psi\rangle = |\psi_{\text{CM}}\rangle|\psi_{\text{rel}}\rangle$. The extra factor of $\frac{1}{2}\hbar\omega$ is just to remove the ground level energy of the center of mass oscillator which would not be present when working in purely relative coordinates.

To be able to implement this we thus need the matrix elements of N in our many-body basis. We have

$$N = \frac{P^2}{2M} + \frac{1}{2}M\omega^2 X^2 - \frac{1}{2}\hbar\omega \quad (2.42)$$

where $X = \frac{1}{n}\sum_j x_j$, $P = \sum_j p_j$ and $M = n_t m$ are the center of mass, total momentum and total mass, respectively. We will now expand the center of mass number operator in the single particle coordinates

$$\begin{aligned} X^2 =& \frac{1}{n_t^2}\left(n_t \sum_j x_j^2 - \sum |x_i - x_j|^2 \right) \\ P^2 =& n_t \sum_j p_j^2 - \sum |p_i - p_j|^2 \end{aligned} \tag{2.43}$$

Thus the shifted Hamiltonian can now be written as

$$\begin{aligned} H_\lambda =& H + \lambda \sum_i \left(\frac{p_j^2}{2m} + \frac{1}{2} m\omega^2 x_i^2 \right) \\ & - \frac{\lambda}{n_t} \left(\frac{1}{2m} \sum_{i,j} |x_i - x_j| + \frac{1}{2} m\omega^2 \sum_{i,j} |p_i - p_j| \right) - (\lambda - 1)\frac{1}{2}\hbar\omega \\ =& H + \lambda H_{\text{osc}} + \lambda V_{\text{osc}} - (\lambda - 1)\frac{1}{2}\hbar\omega \end{aligned} \tag{2.44}$$

Now the structure of this shift is clear. The first part is just like an external harmonic oscillator potential and the second part is like an interaction. Note that this is not the harmonic oscillator interaction mentioned earlier since also the kinetic energy part is included. However, this is an interaction between all particles, thus we can not use the earlier mentioned method to localize the non-zero matrix element. But there is another property we can use, namely that the matrix elements are zero unless the energy of the states are the same which is not true for a general interaction (and particularly not for the point interaction or the harmonic interaction). To see this, consider the interaction term in the single particle coordinates

$$\begin{aligned} \langle n_1, n_2 | V_{\text{osc}} | n_1', n_2' \rangle &= \sum_{N,n,N',n'} \langle n_1, n_2 | N; n \rangle \langle N; n | V_{\text{osc}} | N'; n' \rangle \langle N'; n' | n_1', n_2' \rangle \\ &= \sum_{N,n,n'} \langle n_1, n_2 | N; n \rangle \langle n | V_{\text{osc}} | n \rangle \langle N; n | n_1', n_2' \rangle \end{aligned} \tag{2.45}$$

since it is diagonal in the relative harmonic quantum number n and diagonal and independent of the total harmonic quantum number N. Now, since the overlap brackets are zero unless $n_1 + n_2 = N + n$ and $n_1' + n_2' = N + n$, we have $n_1 + n_2 = n_1' + n_2'$, see section 2.5. This will immensely reduce the number of possible states required when searching for non-zero matrix elements.

2.5 Jacobi to single particle coordinate transformation

Since the Hamiltonian will be written out in single particle coordinates using harmonic oscillator basis states, we need to transform from the relative coordinates in which the interaction is given. Recall that the single particle states are eigenstates of the Hamiltonian

$$H = \frac{p_1^2}{2m} + \frac{1}{2}\omega^2 m x_1^2 + \frac{p_2^2}{2m} + \frac{1}{2}\omega^2 m x_2^2. \tag{2.46}$$

Doing a change of variables to normalized Jacobi coordinates $X = \frac{x_1+x_2}{\sqrt{2}}$ and $x = \frac{x_2-x_1}{\sqrt{2}}$ one obtains

$$H = \frac{p^2}{2m} + \frac{1}{2}\omega^2 m x^2 + \frac{P^2}{2m} + \frac{1}{2}\omega^2 m X^2, \tag{2.47}$$

where the conjugate momenta are $P = \frac{p_1+p_2}{\sqrt{2}}$ and $p = \frac{p_2-p_1}{\sqrt{2}}$. Thus we can define harmonic oscillator eigenstates in Jacobi coordinates as $|N\rangle|n\rangle = |N;n\rangle$ where $|N\rangle$ and $|n\rangle$ are eigenstates to the center of mass part and the relative part of equation (2.47), respectively. It is in these coordinates the two-particle interactions are given (and they are independent of the center of mass coordinate). The transformation between the Jacobi coordinates to the single particle coordinates is in the two-particle subspace

$$|N;n\rangle = \sum_{n_1,n_2} |n_1,n_2\rangle\langle n_1,n_2|N;n\rangle, \tag{2.48}$$

so the interesting quantity is the overlap matrix element. Now recall the definitions of the annihilation operators

$$\begin{aligned}
a_1 =& \sqrt{\frac{m\omega}{2\hbar}}\left(x_1 + \frac{i}{m\omega}p_1\right), \\
a_2 =& \sqrt{\frac{m\omega}{2\hbar}}\left(x_2 + \frac{i}{m\omega}p_2\right), \\
a =& \sqrt{\frac{m\omega}{2\hbar}}\left(x + \frac{i}{m\omega}p\right), \\
A =& \sqrt{\frac{m\omega}{2\hbar}}\left(X + \frac{i}{m\omega}P\right),
\end{aligned} \tag{2.49}$$

from which we see that

$$\begin{aligned}
a =& \frac{a_2 - a_1}{\sqrt{2}}, \\
A =& \frac{a_2 + a_1}{\sqrt{2}}.
\end{aligned} \tag{2.50}$$

Now we can compute the overlap matrix element

$$\begin{aligned}\langle N;n|n_1,n_2\rangle =&\frac{1}{\sqrt{N!n!}}\langle 0;0|\left(\frac{a_2+a_1}{\sqrt{2}}\right)^N\left(\frac{a_2-a_1}{\sqrt{2}}\right)^n|n_1,n_2\rangle\\ =&\frac{1}{\sqrt{N!n!}}2^{-(N+n)/2}\langle 0;0|\sum_{k=0}^{N}\sum_{j=0}^{n}a_1^{k+j}a_2^{N+n-k-j}(-1)^j \\ &\left(\begin{array}{c}N\\k\end{array}\right)\left(\begin{array}{c}n\\j\end{array}\right)|n_1,n_2\rangle,\end{aligned} \tag{2.51}$$

where we used the binomial theorem. Now only terms that have exactly n_1 powers of a_1 and n_2 powers of a_2 will contribute since we need to annihilate exactly n_1 oscillator quanta for particle one and n_2 oscillator quanta for particle two. Thus by forcing $k+j=n_1$ and $N+n-k-j=N+n-n_1=n_2$ and using $a|n\rangle=\sqrt{n}|n-1\rangle$ for the annihilation operators we obtain

$$\begin{aligned}\langle N;n|n_1,n_2\rangle =&\delta_{N+n-n_1,n_2}\sqrt{\frac{n_1!n_2!}{N!n!}}2^{-(N+n)/2}\sum_{k=0}^{N}(-1)^{n_1-k}\left(\begin{array}{c}N\\k\end{array}\right)\left(\begin{array}{c}n\\n_1-k\end{array}\right)\\ =&\delta_{N+n,n_1+n_2}\sqrt{\frac{n_1!n_2!}{N!n!}}2^{-(N+n)/2}\sum_{k=\max\{0,n_1-n\}}^{\min\{N,n_1\}}(-1)^{n_1-k}\\ &\left(\begin{array}{c}N\\k\end{array}\right)\left(\begin{array}{c}n\\n_1-k\end{array}\right)\\ &\equiv m(N,n_1,n_2)\delta_{N+n,n_1+n_2}.\end{aligned} \tag{2.52}$$

Thus, given a matrix element $\langle N;n|V|N',n'\rangle$ in Jacobi coordinates this will in the single particle coordinates be

$$\begin{aligned}\langle n_1,n_2|V|n_1',n_2'\rangle =&\sum_{N,N',n,n'}\langle N;n|V|N',n'\rangle m(N,n_1',n_2')m(N,n_1,n_2)\\ &\delta_{N+n,n_1+n_2}\delta_{N'+n',n_1'+n_2'}.\end{aligned} \tag{2.53}$$

In the case of transforming the two-particle potential the matrix element will be diagonal in and independent of the Jacobi oscillator coordinate N, thus we obtain

$$\begin{aligned}\langle n_1,n_2|V|n_1',n_2'\rangle =&\sum_{N=0}^{\min\{n_1+n_2,n_1'+n_2'\}}\langle n_1+n_2-N|V|n_1'+n_2'-N\rangle\\ &m(N,n_1',n_2')m(N,n_1,n_2).\end{aligned} \tag{2.54}$$

2.6 Description of non-interacting states

In section 2.1.1 we noticed that the matrix elements in relative coordinates of the interaction operator for the contact interaction is zero when any of the two

states are oscillator eigenstates with odd quantum number. This has interesting consequences for the energy spectrum. From Eq. (2.51) we have the expression

$$\langle N;n|n_1,n_2\rangle = \frac{1}{\sqrt{N!n!}}\langle 0;0|\left(\frac{a_2+a_1}{\sqrt{2}}\right)^N\left(\frac{a_2-a_1}{\sqrt{2}}\right)^n|n_1,n_2\rangle. \tag{2.55}$$

If we would switch n_1 and n_2 in this expression we would get the same final result except for a minus sign coming from switching a_1 and a_2. Thus we have

$$\langle N;n|n_1,n_2\rangle = (-1)^n\langle N;n|n_2,n_1\rangle. \tag{2.56}$$

Thus for the matrix element of a completely anti-symmetric state $|(n_1,n_2)\rangle$ we would obtain

$$\langle N;n|(n_1,n_2)\rangle = \frac{1}{\sqrt{2}}\langle N;n|\left(|n_1,n_2\rangle - |n_2,n_1\rangle\right) = [1-(-1)^n]\langle N;n|n_1,n_2\rangle. \tag{2.57}$$

Thus

$$\langle N;n|(n_1,n_2)\rangle = 0, \tag{2.58}$$

if n is even. But from section 2.1.1 we have that

$$\langle n|V|n'\rangle = 0 \tag{2.59}$$

if n or n' is odd. This also implies $V|n'\rangle = 0$ if n' is odd. This together with Eq. (2.58) implies that

$$V|(n_1,n_2)\rangle = \sum_{N,n} V|N;n\rangle\langle N;n|(n_1,n_2)\rangle = 0. \tag{2.60}$$

Now consider again a harmonic oscillator basis state for the whole system

$$|\psi\rangle = |(n_1,\ldots,n_k)\rangle|(m_1,\ldots,m_\ell)\rangle, \tag{2.61}$$

satisfying $H_0|\psi\rangle = E|\psi\rangle$ where H_0 is the non-interacting part of the Hamiltonian and $E = \hbar\omega(\frac{n_\uparrow+n_\downarrow}{2}+n_1+\ldots+n_{n_\uparrow}+m_1+\ldots+m_{n_\downarrow})$. Thus if we form the *totally* antisymmetric state $|(\psi)\rangle$ which is antisymmetric in all particles (basically a state corresponding to all particles being identical fermions) we will get

$$H|(\psi)\rangle = H_0|(\psi)\rangle + V|(\psi)\rangle = H_0|(\psi)\rangle = E|(\psi)\rangle, \tag{2.62}$$

since the interaction will now act in antisymmetric two-particle subspaces which makes this term become zero. Thus all states for a system of $n_\mathrm{t} = n_\uparrow + n_\downarrow$ identical non-interacting fermions will also be eigenstates of the total Hamiltonian of this system (and in particular independent of g). This is not surprising since totally antisymmetric wavefunctions are zero when two particles are at the same point which is exactly where the point-interaction acts. So in the energy spectrum there will be some states that are independent of the interaction strength g and these are precisely these that coincides with the energy states of identical non-interacting fermions.

2.7 Observables

In this section some of the relevant observables will be described.

2.7.1 Occupation numbers

Some simple quantities that are relevant for describing the structure of the eigenstates are the occupation numbers. They basically measure the occupation of every harmonic oscillator state. For one of the subsystems, to calculate the occupation $\langle k \rangle$ of the harmonic oscillator state $|k\rangle$ we will go through all basis states $|n_1, \ldots, n_{n_\uparrow}\rangle$ and add $|\langle \psi | n_1, \ldots, n_{n_\uparrow}\rangle|^2$ to $\langle k \rangle$ if $k = n_j$ for any j. Thus

$$\langle k \rangle = \sum_{(n), k \in n} |\langle (n_1, \ldots, n_{n_\uparrow}) | \psi \rangle|^2. \tag{2.63}$$

Since we are dealing with fermions there will be no states with the quantum number occurring more than once (the contributions should then be multiplied by the number of times it occurs in the basis state). The occupation numbers for the total system are then simply the sum of the occupation numbers in each subsystem.

In experiments it is possible to decrease one of the walls of the trapping potential. This will cause particles to tunnel out from the trap and it is possible to relate the tunnelling frequency to the occupation numbers. Thus this is a particularly interesting observable since it can be measured in experiments.

2.7.2 Density profiles

In this section we will derive expressions for the particle densities. We will start by considering n_t identical fermions. The fundamental definition is the expectation value of the number of identical particles found in the neighbourhood at some position x_0. In the second quantization formalism, this would be the expectation value of the number operator at position x_0, namely[2]

$$N(x_0) = a^\dagger(x_0) a(x_0). \tag{2.64}$$

Here $a^\dagger(x_0)$ creates a particle at position x_0 and $a(x_0)$ annihilates a particle at position x_0. The expectation value of this quantity is now

$$\rho(x_0) = \langle \psi | N(x_0) | \psi \rangle = \langle \psi | a^\dagger(x_0) a(x_0) | \psi \rangle. \tag{2.65}$$

The annihilation operator will annihilate one particle so this is really a scalar product of two $n_\mathrm{t} - 1$ particle states since $(a(x_0)|\psi\rangle)^\dagger = \langle \psi | a^\dagger(x_0)$.

A general annihilation operator for a state χ acts on a many particle basis state $|\alpha_1, \ldots, \alpha_{n_\mathrm{t}}\rangle$ as

$$a(\chi)|\alpha_1, \ldots, \alpha_{n_\mathrm{t}}\rangle = \sum_{j=0}^{n_\mathrm{t}} \langle \chi | \alpha_j \rangle \xi^{j-1} |\alpha_1, \ldots, \alpha_{j-1}, \alpha_{j+1}, \ldots, \alpha_{n_\mathrm{t}}\rangle, \tag{2.66}$$

where $\xi = 1$ for bosons and $\xi = -1$ for fermions and the remaining state is a sum over $n_\mathrm{t} - 1$-particle states with the state α_j removed. In our case the basis states are the harmonic oscillator eigenstates and ψ will be a linear combination of these states,

$$|\psi\rangle = \sum_{(n)} C_n |(n_1, \ldots, n_{n_t})\rangle, \tag{2.67}$$

where the brackets now emphasizes that this is an antisymmetrized state and the sum is thus only over states with $n_1 > \ldots > n_{n_t}$. n is here a collective index representing the set $\{n_1, \ldots, n_{n_t}\}$. Inserting this expansion into equation (2.65) and using equation (2.66)

$$\begin{aligned}\rho(x_0) = &\sum_{nn'} C_n^* C_{n'} \sum_{i=1,j=1}^{n_t} \langle n_j|x_0\rangle \xi^{j-1} \langle x_0|n_i'\rangle \xi^{i-1} \\ &\langle n_1, \ldots, n_{i-1}, n_{i+1}, \ldots, n_{n_t}|n_1', \ldots, n_{j-1}', n_{j+1}', \ldots, n_{n_t}'\rangle.\end{aligned} \tag{2.68}$$

The last bracket is a scalar product of two orthonormal many-body basis states so they have to be equal, meaning that these two $n_\mathrm{t} - 1$-particle many-body states has to contain exactly the same single particle states. Thus the only contributing terms in the double sum over the collective indices n and n' are over the products where n and n' have $n_\mathrm{t} - 1$ identical oscillator states. Note however that for the terms where $n = n'$ the sum over i, j will not vanish but give n_t contributions, one time for each $i = j$. Denoting the condition that n and n' has exactly $n_\mathrm{t} - 1$ identical single particle states by $|n - n'| = 1$ we have

$$\rho(x_0) = \sum_{|n-n'|=1} C_n^* C_{n'} \phi_{n_i}^*(x_0) \phi_{n_j'}(x_0) \xi^{j-i} + \sum_n |C_n|^2 \sum_{i=0}^{n_t} |\phi_{n_i}(x_0)|^2, \tag{2.69}$$

where i and j in the first sum now are the indices for the states that are not among the $n_t - 1$ oscillator states in n and n' that are forced equal by the orthonormality condition. Formula (2.69) is the final expression for a density of a system of identical system and we can use that to calculate the density of the subsystems. The sum over n, n' should then be over all pairs of many-body states that differ with one quantum number in the part of the basis in the particular subsystem. The total density is then the sum of the densities of the two subsystems. Efficient ways of locating pairs of states that differs with one single particle state will be discussed in section 3.

2.7.3 Momentum space

The momentum space densities can be obtained by using that the Hermite functions are eigenfunctions under the Fourier transform, i.e. we have

$$\frac{1}{\sqrt{2\pi\hbar}} \int_{-\infty}^{\infty} \exp(-ikx/\hbar) \phi_n(x) = (-i)^n \phi_n(k). \tag{2.70}$$

Thus the expression (2.69) changes to

$$\rho(x_0) = \sum_{|n-n'|=1} C_n^* C_{n'} \phi_{n_i}^*(x_0)\phi_{n'_j}(x_0)\xi^{j-i}(-i)^{n_i-n'_j} + \sum_n |C_n|^2 \sum_{i=0}^{n_t} |\phi_{n_i}(x_0)|^2. \tag{2.71}$$

The imaginary unit might look a bit troublesome but the result is definitely still real. Let $n_{\text{rel}} = n_1 - n'_1$. Then we have

n_{rel} mod 4	0	1	2	3
$(-i)^{n_{rel}}$	1	$-i$	-1	i

Now we see that the imaginary terms will not cause any trouble because the term with n_{rel} would be cancelled by the one with $-n_{\text{rel}}$ since one will be multiplied with $-i$ and the other by i and the expression is otherwise symmetric. In conclusion, the only modification needed when going from the coordinate space density to the momentum space density is to change sign of the terms that have $n_{rel} \equiv 2 \bmod 4$.

2.7.4 Pair correlation function

The pair correlation function measures the probability of finding a particle at position x_2 given we have one at position x_1. For systems with translational symmetry this could be written as a function of $x_2 - x_1$ but this is not the case in this system because of the trapping potential. Thus we will be dealing with a function of two variables. For two particles this would just be the total probability density for the two particles in single particle coordinates. For a $1 + N$ particle system this could be interpreted as the density of the N-particle system given that the lonely particle is found at some position x_1. We will only look at correlations between two particles from different subsystems. In the formalism of second quantization, the pair correlation function is[2]

$$g(x_1, x_2) = \langle\psi|a^\dagger(x_1)b^\dagger(x_2)b(x_2)a(x_1)|\psi\rangle. \tag{2.72}$$

Here a and b are annihilation operators for particles of different spins. Now we expand $|\psi\rangle$ in the complete many-body basis

$$|\psi\rangle = \sum_{n,m} C_{n,m}|n_1, \ldots, n_{n_\uparrow}\rangle|m_1, \ldots, m_{n_\downarrow}\rangle. \tag{2.73}$$

This gives

$$\begin{aligned} b(x_2)a(x_1)|\psi\rangle = &\sum_{n,m} C_{n,m} \sum_{i=1}^{n_\uparrow}\sum_{j=1}^{m_\downarrow} \langle x_1|n_i\rangle\langle x_2|m_j\rangle\xi^{i+j} \\ &|n_1, \ldots, n_{i-1}, n_{i+1}, \ldots, n_{n_\uparrow}\rangle|m_1, \ldots, m_{j-1}, m_{j+1}, \ldots, m_{n_\downarrow}\rangle. \end{aligned} \tag{2.74}$$

Inserting this into equation (2.72) we will obtain the expression

$$g(x_1, x_2) = \sum \phi_{n_i} \phi_{n'_{i'}} \phi_{m_j} \phi_{m'_{j'}} C_{n,m} C_{n',m'} \xi^{i+j+i'+j'}, \tag{2.75}$$

where the sum goes over all configurations (n, n', m, m') where m, m' are collective indices for one subsystem and n, n' are collective indices for the state in the other subsystem. Only configurations which differ with at most one quantum number in both systems are summed over and i, j, i', j' are the indices of the differing states. The terms where $n = n'$ or $m = m'$ are understood to be inside the sum and in these cases the indices $i = i'$ and $j = j'$, respectively, are summed over.

2.8 Effective interaction

A very common problem in physics is handling strongly coupled systems. Here it arises in the sense that the matrix elements of the interaction for high harmonic oscillator basis states are very big. Thus we need to include many basis states to reach convergence in the eigenvalues when truncating the Hilbert space to represent the Hamiltonian as a matrix. The subspace spanned by the truncated basis will be denoted M and its complement is M^c. To solve this problem we will do a unitary transformation on the Hamiltonian to obtain an effective interaction which will make the results converge faster. The idea is that this transformation should remove all the couplings between M and M^c (i.e off block diagonal matrix elements $\langle\alpha|H|\beta\rangle$ where $|\alpha\rangle \in M$ and $|\beta\rangle \in M^c$). This would split the Hamiltonian into a product of two operators $H_M \otimes H_{M^c}$ acting on the Hilbert space $M \otimes M^c$, and these could then be diagonalized separately and one could then just focus on the model space which will include the lowest energy values. However, finding such a unitary transformation would be just as troublesome as diagonalizing the matrix itself so this is where an approximation comes in. Assuming that we start with a Hamiltonian on the form

$$H = H_0 + V_2^{eff} \tag{2.76}$$

where H_0 includes the external potential and kinetic energy terms and V includes all two-particle interactions. However, when doing a unitary transformation on this Hamiltonian it will not be possible to keep it on this particular form but rather

$$H_{eff} = H_0 + V_2^{eff} + V_3 + \ldots + V_n \tag{2.77}$$

where V_j is a j-particle interaction and n are the number of particles in the system. The approximation we will do is to neglect all the induced many-body interactions and force the Hamiltonian on the form $H_{eff} = H_0 + V_2^{eff}$. This is equivalent to doing the unitary transformation in the two-body subspace (i.e on a two-particle Hamiltonian) that decouples the model space from its complement and then just use the effective interaction obtained here in the many-body Hamiltonian. In the limit of a very large model space this will be an exact unitary transformation since then the bare interaction is the same as the effective

interaction. Now there is only one degree of freedom (the relative motion) in the two-particle subsystem so this is a great simplification. We also have exact analytical solutions available in the two-body subsystem which turns out to be very advantageous.

Let P denote the projection operator to the model space and Q the projection operator to the complement such that $P+Q=1$. We thus wish to find a unitary transformation, written as $U = e^S$ where S is antihermitian, that transforms the Hamiltonian to

$$H_{eff} = e^{-S} H e^{S} \tag{2.78}$$

The condition of removing the couplings is then

$$QH_{eff}P = 0 \tag{2.79}$$

which is equivalent to saying that matrix elements of H between a state from M and one from M^c will vanish.

The following equation is an explicit formula for the unitary transformation used[9]

$$H_{\text{eff}} = \frac{P + P\xi Q}{\sqrt{P + \xi^\dagger \xi}} H \frac{Q\xi P + P}{\sqrt{P + \xi^\dagger \xi}}. \tag{2.80}$$

When restricting ourselves to a two-particle subspace we get[9]

$$H^{(2)}_{\text{eff}} = (A^{-\dagger}A^{-1})^{-1/2} A^{-\dagger} E A^{-1} (A^{-\dagger}A^{-1})^{-1/2} \tag{2.81}$$

where E is the diagonal matrix with eigenvalues from the two-particle subspace and A is a matrix containing the corresponding eigenvectors.

2.8.1 Convergence properties

When doing the unitary transformation in the two-particle subspace we specify a model space cutoff $n_{\max}$ on the relative harmonic oscillator coordinate. When doing the transformation the correlations are moved from the full matrix into this smaller model space and all matrix elements higher than this $n_{\max}$ are taken to be zero. In the two-particle system, if we are working in relative coordinates, it is then obvious that diagonalizing this effective Hamiltonian in the model space gives the same eigenvalues as diagonalizing it in a larger space (since all extra matrix elements are zero anyway). However, when solving the many-body problem in single particle coordinates it is not as obvious how many oscillator states we need to include. Lets say our unitary two-body cutoff is $n_{\max}$ and the cutoff on the total energy (in harmonic oscillator units) is n_{tot}. The we recall equation 2.54 of the transformation from relative coordinates to single particle coordinates

$$\langle n_1, n_2|V|n_1', n_2'\rangle = \sum_{N=0}^{\min\{n_1+n_2, n_1'+n_2'\}} \langle n_1 + n_2 - N|V|n_1' + n_2' - N\rangle \\ m(N, n_1', n_2')m(N, n_1, n_2). \tag{2.82}$$

The potential is zero for Here we see that high values of n_1, n_2, n_1', n_2' will still give non-zero contributions since the sum is over interaction matrix elements with relative quantum numbers less than $\min\{n_1 + n_2, n_1' + n_2'\}$. More specifically, for terms in the sum to be non-zero, N must satisfy

$$\max\{n_1 + n_2, n_1' + n_2'\} - n_{\max} \leq N \leq \min\{n_1 + n_2, n_1' + n_2'\}. \tag{2.83}$$

Then we see that if the difference between bra's and the ket's energies is sufficiently big compared to the two-body cutoff $n_{\max}$, namely if $|n_1+n_2-n_1'-n_2'| > n_{\max}$, all terms will be zero. Thus the couplings between low energies and high energies is still small so to obtain the lowest eigenenergies we should not have to include that many states above the two-body cutoff. As we see in Fig. 2.1 the correction of including states with total energy above $n_{\max}$ is very small. The energy seems to decrease linearly below the two-body cutoff but above $n_{\max}$ it converges very fast. This is expected since below this cutoff there will be some matrix elements in the potential that will not be included at all. In numerical simulations we will typically have $n_{\text{tot}} - n_{\max} \in [2, 10]$.

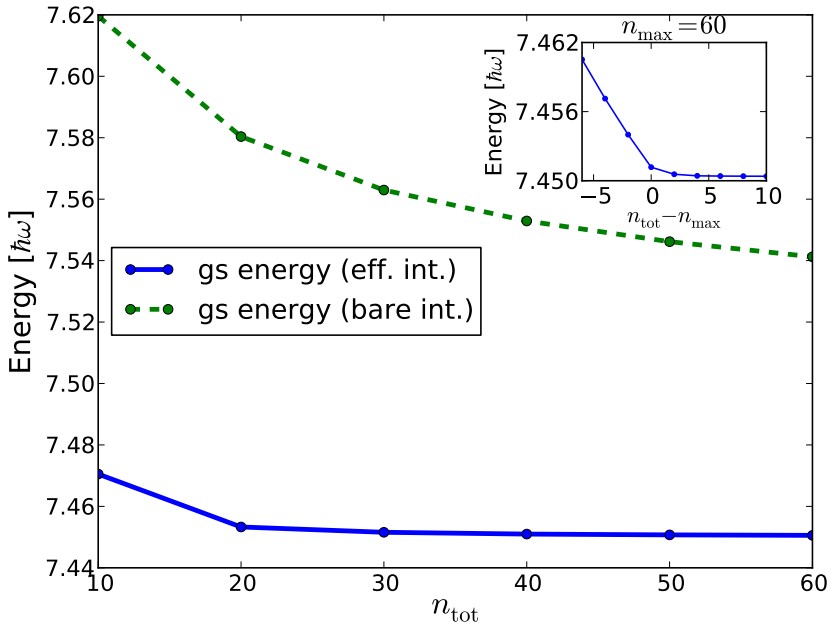

Figure 2.1: Convergence of energy with respect to increased model space where $n_{\mathrm{tot}} - n_{\mathrm{max}} = 2$ is kept fixed for the ground state of the 1+3 particle system at $g = 100$. The small plot shows energy convergence as a function of $n_{\mathrm{tot}} - n_{\mathrm{max}}$ while $n_{\mathrm{tot}} = 60$ is kept fixed.

Chapter 3

Implementation

In this section some parts of the implementation will be discussed. The main focus for this project has been on developing a fast and effective algorithm to generate the matrix representation of the Hamiltonian.

3.1 Representation of the many-body states

A many-body basis state in our truncated Hilbert space basis will be labelled by indices. As a consequence, we can represent an arbitrary state as a vector where the elements are the expansion coefficients for the many-body states. There is no obvious way to index the states because each state is a set of unordered quantum numbers, see section 2.2.1, but the way that the states are indexed is not important. However the way the states are indexed can matter for efficient computer implementations. The states will at least be ordered in energy so that a state with higher energy has a higher index making truncation in the Hilbert space easier.

3.2 Creating the Hamiltonian

As was explained in section 2.2.2, the non-zero elements originating from the interaction are those where the bra and ket have at most two quantum numbers different, one from each spin species (due to the fact that the interaction only acts between particles with different spin). To find all such pairs, we can first consider basis states for each spin species separately and find all pairs that differ by at most one single particle quantum number. All possible pairs of basis states for the full system can then be obtained by combining pairs in the two subsystems. Thus we will focus on basis states for one subsystem. To find all pairs of states that differ by at most one single particle quantum number by just going through all basis states would be very slow and inefficient. A better way is to, for each basis state, generate all other basis states that satisfy this criteria and then find the indices for these states.

3.2.1 Single particle jumps

To generate all required states, one can systematically change each of the single particle quantum numbers to generate all other states that differ with at most one number. This is done separately within each spin species and the full many-body states are then given by all tensor product combinations of few-body states from each spin species. For example consider the three particle few-body state (for one spin species)

$$|(7, 5, 2)\rangle \tag{3.1}$$

We would start by changing the first index to generate all states of the form

$$|(m, 5, 2)\rangle \tag{3.2}$$

To fulfill the Pauli principle, m takes the values 1, 3, 4, 6, 7,.... We also need to reorder the quantum numbers in decreasing order to be consistent with our sign convention and this will result in a possible sign change equal to the sign of the permutation needed to perform this reordering. After this all states resulting from changing the other two indices (5 and 2) will be generated. The next problem is then to find the index of these new states, since the mapping from index to many-body state is very hard to invert. For this it is very convenient to use hash tables. All such pairs of few-body states, together with a possible sign change, will then be stored to be used later when generating the matrix.

3.2.2 Hash tables

A hash table is a way to look up the index of an ordered collection of objects. The idea is to compute the so called hash function of the object. The hash function is a function that takes as it's argument an object (in this case a few-body state or a many-body state) and gives back a single number (called the key) that can be used as an alternative index. Thus we can now store the states in a new table, with indices that are very easy to compute. One might ask the question why we can't just use this number to index our states in the first place. The reason is that the whole point of the hash function is that it should be fast to compute, and that comes with the price that it is not one-to-one. There is no guarantee that it will be surjective and there is also very likely that two objects can have the same key. Thus it is necessary to deal with collisions where two states have the same key.

The easiest way is just to loop through all states with the same key and then compare with the states one is looking for. This search algorithm is of course very inefficient, but if the hash function is chosen in a smart way collisions will not appear very often and the time required for this search is very small. In other words, we would like the hash function to be as "random" as possible to minimize the frequency of collisions. To reduce the risk of periodic behaviour in the hash function which could result in collisions it is beneficial to make the size of the table a prime number.

3.3 Precomputed coordinate transformation matrix elements

The overlap matrix elements $\langle N, n | n_1, n_2 \rangle$ will be precomputed and stored on disk to save computation time. However, if we saved the matrix elements for each quantum number in $\{0, 1, \ldots, n_{\text{tot}}\}$ this would scale as n_{tot}^4, where n_{tot} is the highest used single particle quantum number induced by the many body cutoff. Thus it is relevant to try to use the properties of these matrix elements to only store non-zero elements. First of all, these matrix elements are only non-zero if $N + n = n_1 + n_2$. Thus we only need to specify N, n_1, n_2 when specifying a matrix element. Furthermore, since $n \geq 0$ we need to have $N \leq n_1 + n_2$. Thus, we only need to store matrix elements for $n_1, n_2 \in \{0, 1, \ldots, n_{\text{tot}}\}$ and $N \in \{0, 1, \ldots, n_1 + n_2\}$ for each n_1, n_2. Now the next problem is how to calculate the position of a matrix element in a one-dimensional list. If we would have generated elements for all $N \in \{0, 1, \ldots, n_{\text{tot}}\}$ the index is just

$$i = n_1(n_{\text{tot}} + 1)^2 + n_2(n_{\text{tot}} + 1) + N$$

assuming that n_1 is looped over in the outermost loop, n_2 in the second outermost and N in the innermost and the list index starts at zero. Instead we will have the following expression

$$\begin{aligned} i =& \sum_{n_1'=0}^{n_1-1} \sum_{n_2'=0}^{n_{\text{tot}}} (n_1' + n_2' + 1) + \sum_{n_2'=0}^{n_2-1} (n_1 + n_2' + 1) + N \\ =& n_{\text{tot}} n_1 (n_1 - 1)/2 + n_1 n_{\text{tot}} (n_{\text{tot}} + 1)/2 + n_1 (n_{\text{tot}} + 1) \\ & + n_1 n_2 + n_2 (n_2 - 1)/2 + n_2 + N \end{aligned} \tag{3.3}$$

3.4 Diagonalization

To diagonalize the matrix we have used the Lanczos algorithm which is essentially an extension of the power method. In the power method one notes that if x_0 is a random vector, then $x_n / ||x_n||$ defined by $x_{n+1} = A x_n$ converges to the eigenvector v_1 corresponding to the largest eigenvalue λ_1 of A (unless x_0 is orthogonal to v_1 but this should almost never happen). This comes from the fact that the eigenvectors of A form a complete basis, thus we can expand x_0 as

$$x_0 = \sum_i c_i v_i \tag{3.4}$$

Thus the vectors defined by $x_{n+1} = A x_n$ are equal to

$$x_n = \sum_i c_i \lambda_i^n v_i \tag{3.5}$$

Thus for large n this approaches the eigenvector corresponding to the largest eigenvalue.

In this method the vectors in each step are discarded. The idea with the Lanczos method is to improve this algorithm by using information from these discarded vectors. Thus we form the so called *Krylov matrix*

$$K_n = \begin{bmatrix} x_0 & Ax_0 & A^2x_0 & \dots & A^{n-1}x_0 \end{bmatrix} , \tag{3.6}$$

whose column vectors span the *Krylov subspace* $\mathcal{K}_n$. From these vectors we can use the Gram-Schmidt process to extract an orthogonal basis and these eigenvectors will then approximate the eigenvectors corresponding to the n largest eigenvalues of A. To motivate this, consider

$$x_{n-2} = \sum_i c_i \lambda_i^{n-2} v_i \tag{3.7}$$

In the Gram-Schmidth process, we will make this ortogonal to $\hat{v}_1 = A^{n-1}x_0$ and create $\hat{v}_2$. Since $\hat{v}_1$ approximates v_1 we expect this step to be roughly equal to removing the term λ_1^{n-2} from (3.7). Thus the most important contribution to $\hat{v}_2$ will be $\lambda_2^{n-2}v_2$ and thus this vector approximates v_2 (up to a normalization). By the same argument we can obtain approximate solutions $\hat{v}_3, \dots, \hat{v}_n$ to the rest $n-2$ eigenvectors as well. However, we expect that the approximation of v_j will get worse for higher j.

The problem with the above method is that is is not numerically stable and one will have to refine this algorithm by using the stabilized Gram-Schmidth process. This algorithm is called the Arnoldi method and the Lanczos method is this algorithm specialized to symmetric matrices.For a more detailed description of the Lanczos algorithm see [6, 5].

Chapter 4

Results

In this section some of the results will be presented. We will start by looking at the analytical results of the occupation numbers of the two-particle system since they are easier to interpret than for systems with more particles. We will then continue to results of systems with more particles obtained form the numerical simulations.

4.1 1+1 system

In Fig. 4.1 the total occupation numbers of the 1+1 system as a function of interaction is shown. The energy is also plotted in the same graph. This is basically an analytic result, except that there is a cutoff when transforming from the analytic formula for the wavefunctions in relative coordinates to single particle coordinates. On the repulsive side it starts in the ground state with both particles in the lowest harmonic oscillator eigenstate thus the energy is $\frac{\hbar\omega}{2}$ (remember that the center of mass ground energy of $\frac{\hbar\omega}{2}$ is removed). It then evolves to a state with energy $\frac{5\hbar\omega}{2}$ and thus we need to move the particles in total two levels up in the harmonic oscillator potential (which is also consistent with parity conservation). However, looking at the occupation numbers it is clear that the eigenstate is a linear combination of the state with both particles in the second oscillator level and the (symmetrized[1]) state with one in the lowest level and one in the third level, namely

$$\frac{|0\rangle|2\rangle + |2\rangle|0\rangle}{2} + \frac{|1\rangle|1\rangle}{\sqrt{2}}. \tag{4.1}$$

Tensor products of single particle states are in general not the eigenstates of the interacting Hamiltonian when $g \to 0$. The degenerate energy levels will split up when the interaction is turned on, but there is no guarantee that they will

[1] If it would be the antisymmetrized state, then by symmetry also the state where we change the sign on this state would be an eigenstate, leading to $|1\rangle|1\rangle$ also being an eigenstate which is not possible.

split up into the product states of single particle states. In fact, the eigenstates (to non-degenerate energy levels) must be eigenstates of the center of mass number operator (see section 2.4). Thus this can not happen since the product states are not eigenstates of the center of mass number operator. The correct eigenstates at the $g \to 0$ limit for a certain degenerate energy level can be obtained by zeroth order perturbation theory and are exactly the set of states that diagonalize the interaction operator in the subspace spanned by the states at this energy level[13].

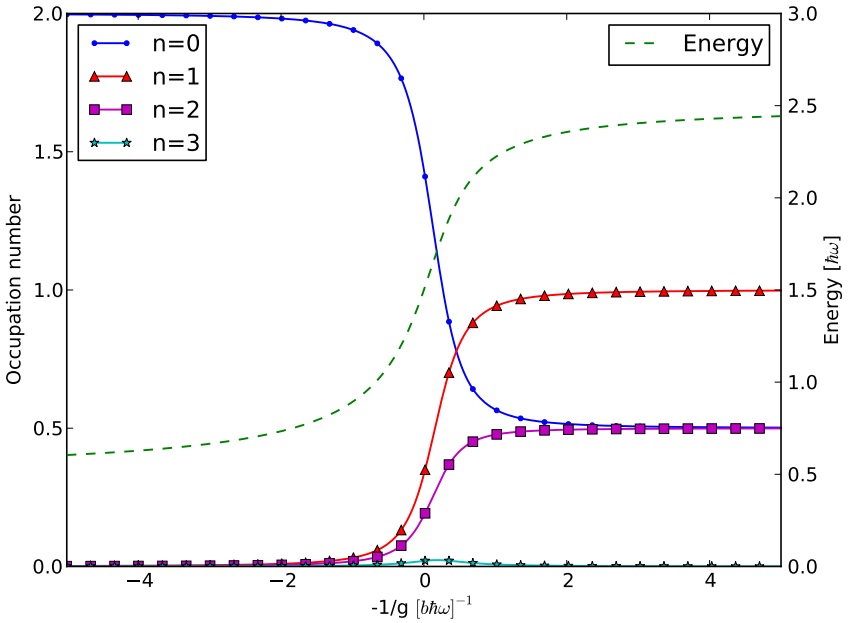

Figure 4.1: Total occupation numbers and energy for the ground state on the repulsive side in the 1+1 system as it evolves through the resonance.

4.2 2+1 system

In this section we will carefully study the system where one subsystem contains one particle and the other subsystem contains two particles. In Fig. 4.2 the energy spectrum as a function of the interaction is shown. There are both differences and similarities with the system of two distinguishable fermions. First of all, we note that the energy spectrum at infinite interaction coincides with the energy spectrum for three indistinguishable fermions, although every energy level is degenerate. On the attractive side, we have infinitely many states that diverge to minus infinity, which should be compared to the two particle case where there was only one such state. This is reasonable since we can imagine a state composed of the diverging state in the 1+1 case and then a spectator

particle which can be in any oscillator level. Thus we should have one diverging state for every energy which is exactly what we see. Although this gives the correct number of states it is not a completely correct description since all three particles are interacting.

There are also many states that connect at infinite interaction, and since they also connect at zero interaction it is possible to follow a state arbitrarily high up in the spectrum. As explained earlier it is possible to connect these states in experiments. By mapping g to the finite interval $[-\pi, \pi]$ by $g \to \arctan(g)$ it is possible to visualize this on a cylinder, see Fig. 4.3. Here the ground state and its evolution up in the spectrum has been boldfaced. It is not obvious which state it connects to at zero interaction and to determine this it is necessary to demand continuity in the wavefunction.

In Fig. 4.2 the spectrum of two particles plus a constant energy shift of $\frac{5\hbar\omega}{2}$ is displayed. One can observed that this resembles some of the curves in the 2+1 spectrum. This is because if the main interaction energy comes from only two particles forming a molecular-like state, while the third one is far away and thus its interaction energy is low, the energy spectrum should look like the two particles system's spectrum plus the potential energy of the spectator particle. However, for excited states, we see a discrepancy between the two-particle spectrum and the energy levels of the three-particle spectrum and thus all three particles interact with each other.

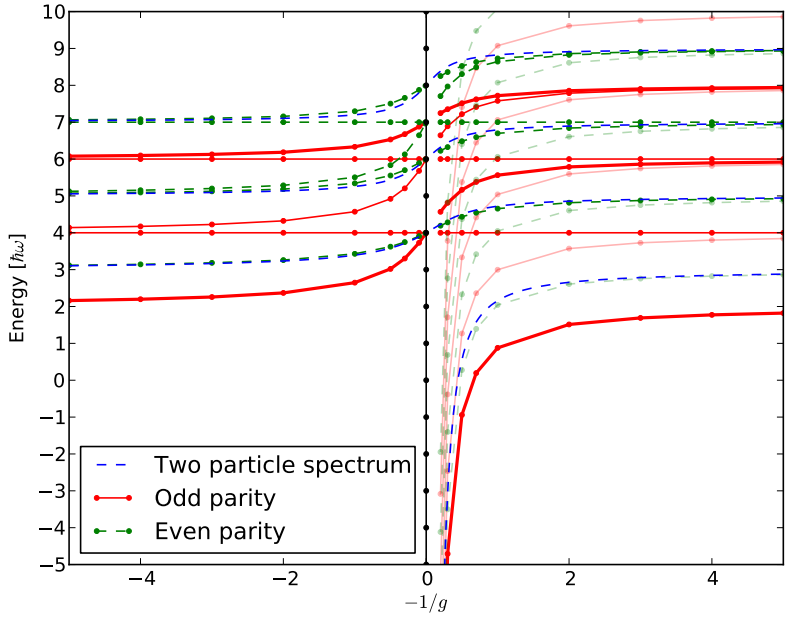

Figure 4.2: Energy spectrum of the 2+1 system. The energy spectrum from the Busch model, shifted with an energy shift of $\frac{5\hbar\omega}{2}$ is also shown and can be observed to match some of the energy levels very well.

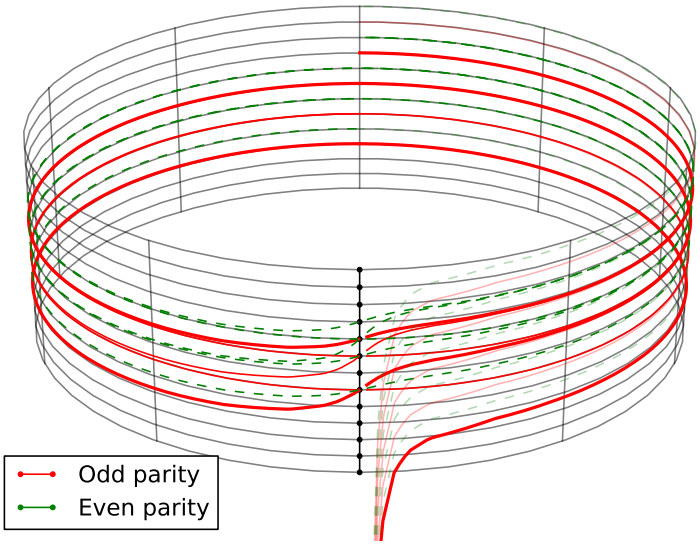

Figure 4.3: Energy spectrum of the 2+1 system wrapped on a cylinder.

The density profiles of the spin-separated particle subsystems and the total density of the lowest odd parity state and the lowest even parity state for different interactions are shown in Fig. 4.4 and Fig. 4.5, respectively. In Fig. 4.6 the momentum space densities of the lowest odd parity state are shown. In all plots the non-interacting second lowest odd parity state is also shown and when $g \to \infty$ these all have the same energy. The densities are normalized to equal the number of particles in the system. It is interesting that the total coordinate space densities all converge to the same value when $g \to \infty$, even though the densities of the subsystems do not but in momentum space none of the densities converge to the non-interacting state. This is perfectly fine, since the short range repulsion will cause particles to avoid each other in *position space only* and thus should resemble the Pauli principle in position space. Nothing can really be said about the distribution in momentum space form this argument.

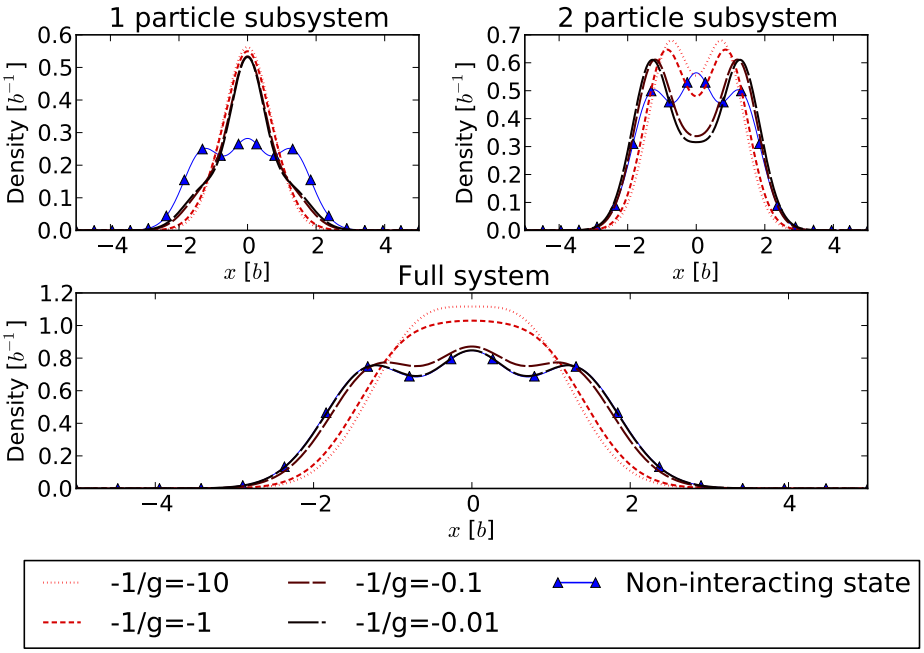

Figure 4.4: Coordinate space particle densities of the lowest odd parity state of the 2+1 particle system for different interactions. Darker colored curves represent stronger interaction and the blue curve is the density of the second lowest odd parity state which is a non-interacting state, independent of the interaction.

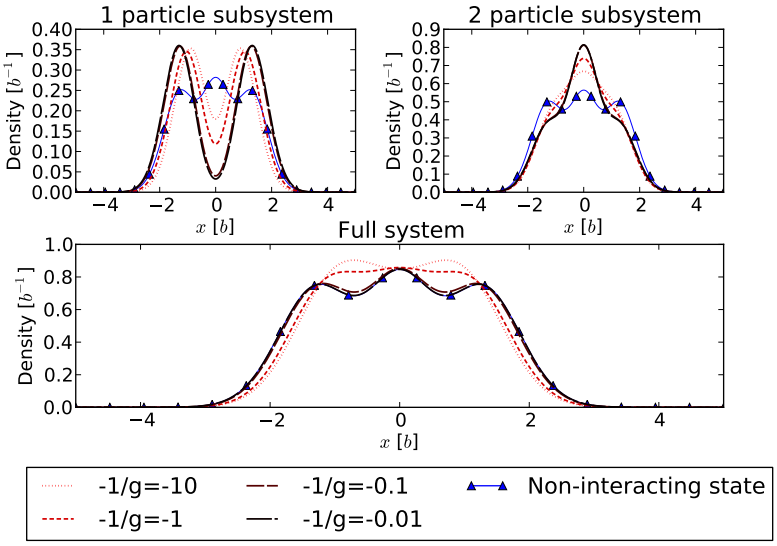

Figure 4.5: Coordinate particle densities of lowest even parity state of the 2+1 particle system for different interactions. Darker colored curves represent stronger interaction and the blue curve is the density of the second lowest odd parity state which is a non-interacting state, independent of the interaction.

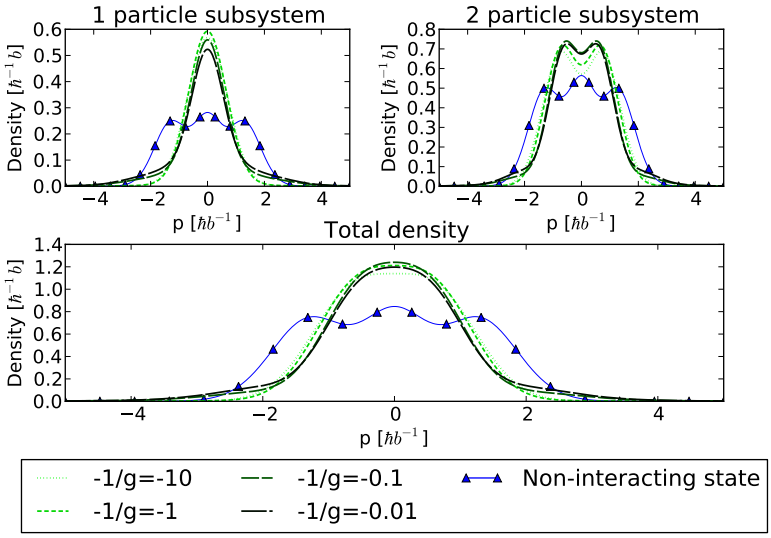

Figure 4.6: Momentum space particle densities of the lowest odd parity state of the 2+1 particle system for different interactions. Darker colored curves represent stronger interaction and the blue curve is the density of the second lowest odd parity state which is a non-interacting state, independent of the interaction.

In Fig. 4.7 the occupation numbers for the two states are shown as a function of g. We can see that the occupation numbers connect at infinite interaction. However, the occupation numbers approach non-trivial values and can not be matched with a state of identical fermions which again can be connected to the fact that the strong repulsive interaction is like a Pauli principle in position space only. Of course the wavefunctions of different states must be orthogonal to each other so then the expansion coefficients can not be equal. The occupation numbers show that the state starts out with two particles in the lowest oscillator level and one in the second level. After the state has gone to through the resonance the eigenenergy approaches $6\hbar\omega$ which means that there has to be four excitations from the ground level and the resulting state is a linear combination of all such states causing the non-trivial occupation numbers just as in the 1+1 case.

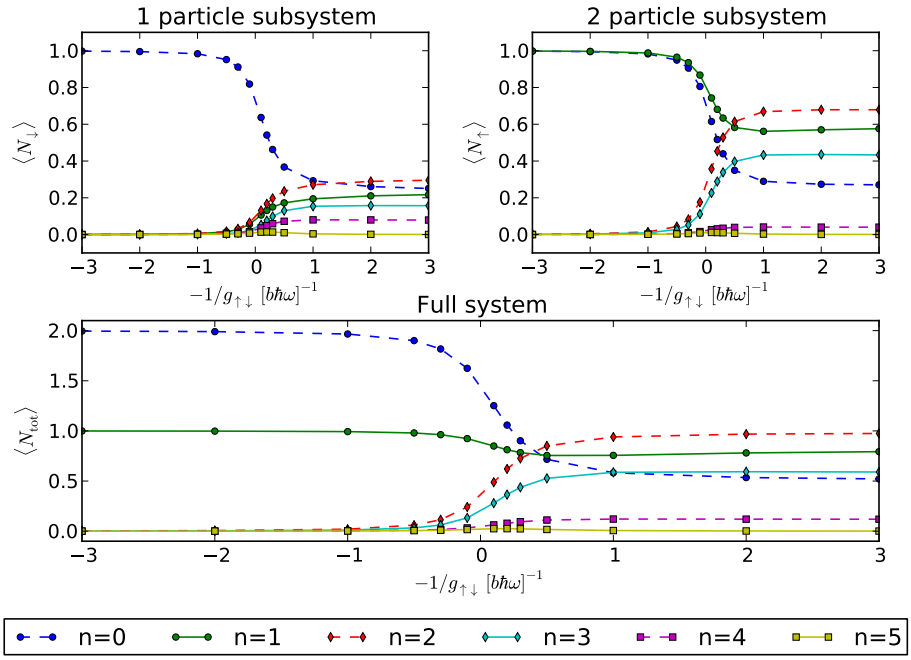

Figure 4.7: Occupation numbers for the 2+1 system as a function of g for the lowest odd parity state.

In Fig. 4.8 and 4.9 the pair correlation functions for the two lowest states are shown, compared with the non-interacting state. These shows the correlation of the densities between the two subsystems. For a $1 + n$ particle system it can be interpreted as the conditional density of the n particle system given that the single particle is measured at a certain position. From these figures one can also draw the same conclusion as before, that for the odd parity state the single particle is pushed to the middle and the two particles are pushed to the sides, while for the even parity state it is the opposite. However, the limit of the two states correlation function is not the same as the non-interacting ones.

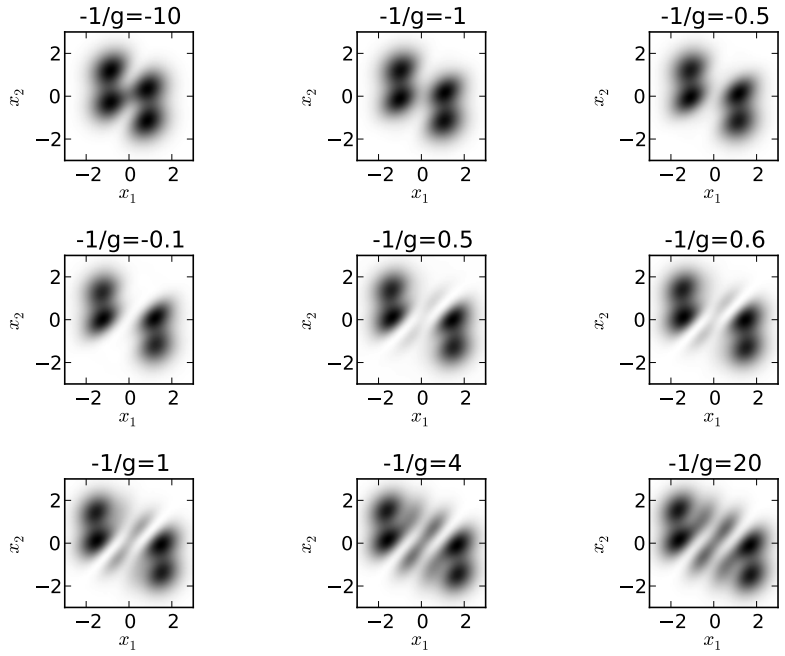

Figure 4.8: Pair correlation function for the lowest even parity state on the repulsive side followed through the resonance $g \to \infty$ in the 2+1 particle system.

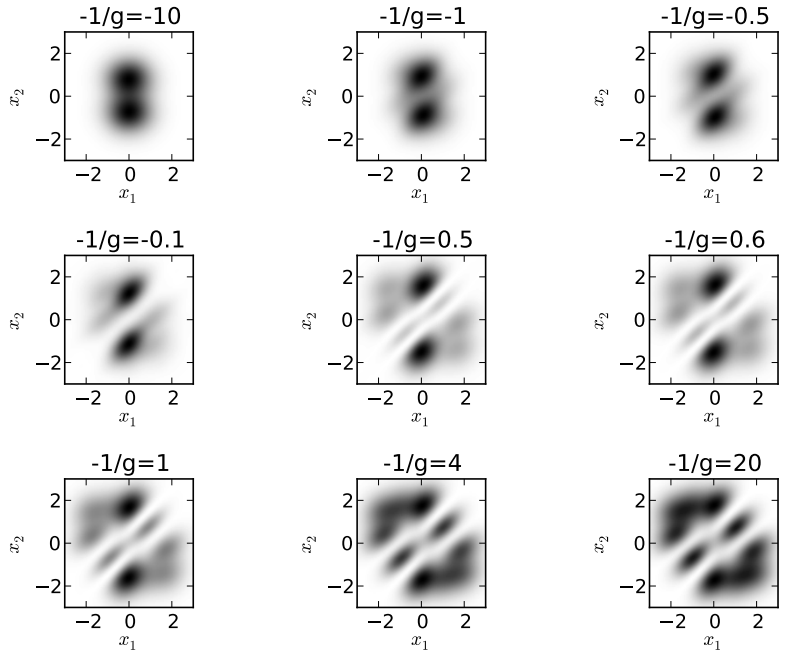

Figure 4.9: Pair correlation function for the lowest odd parity state on the repulsive side followed through the resonance $g \to \infty$ in the 2+1 particle system.

When the interaction increases on the repulsive side the particles from different subsystems get pushed away from each other which is seen as a band around $x_1 = x_2$ where the correlation is zero. When we pass through the resonance, a band along $x_1 = x_2$ starts to get present.
It is also interesting to look at the different energy contributions. In Fig. 4.10 the expectation values of the different parts of the Hamiltonian are shown as a function of g for the lowest odd parity state on the repulsive side. When the interaction starts to increase the interaction energy gets bigger and thus increasing the total energy. The particles also get pushed away from each other to reduce the interaction energy which can be seen in the pair correlation function and from the fact that the potential energy part increases. At around $g = 2$ the potential and kinetic energy increases significantly. Now the particles separation increases fast enough to overcome the increase in g and thus making the expectation of the interaction energy decrease in total. When $g \to \infty$ the interaction energy goes to zero meaning that the particles are now completely separated from each other and fermionization has occurred. There is also an interesting separation between the potential energy and the kinetic energy. For a harmonic oscillator eigenstate these would be equal but when we increase the interaction the particles get pushed to the sides thus increasing the potential energy and not the kinetic energy. Then when the particles separation gets bigger the short range interaction does not affect the particles anymore thus the

state starts to resemble a harmonic oscillator eigenstate and at fermionization the potential energy and kinetic energy are equal. On the attractive side similar things happen.
In Fig. 4.11 the different energy contributions for the lowest odd parity state on the attractive side are displayed. In this state the particles collapse as the interaction gets stronger and stronger and the interaction energy and total energy diverges to minus infinity. It can also be noted that the potential energy decreases which is expected since the particles collapse at the point $x_1 = x_2 = 0$, see Fig. 4.12. The kinetic energy also increases. This could be interpreted as an analogy to a classical system of two bodies with an attractive interaction (for example two stars). If the interaction increases and the bodies move closer to each other, their momentum must increase to sustain a stable bound system. It is also interesting to note that the potential energy does not go to zero. Thus the process should be interpreted as two particles collapsing in the potential minimum causing a diverging interaction energy and a zero potential energy while the third particle, which has to obey the Pauli principle with respect to one of the other two particles, must be further away and thus has a non-zero potential energy.

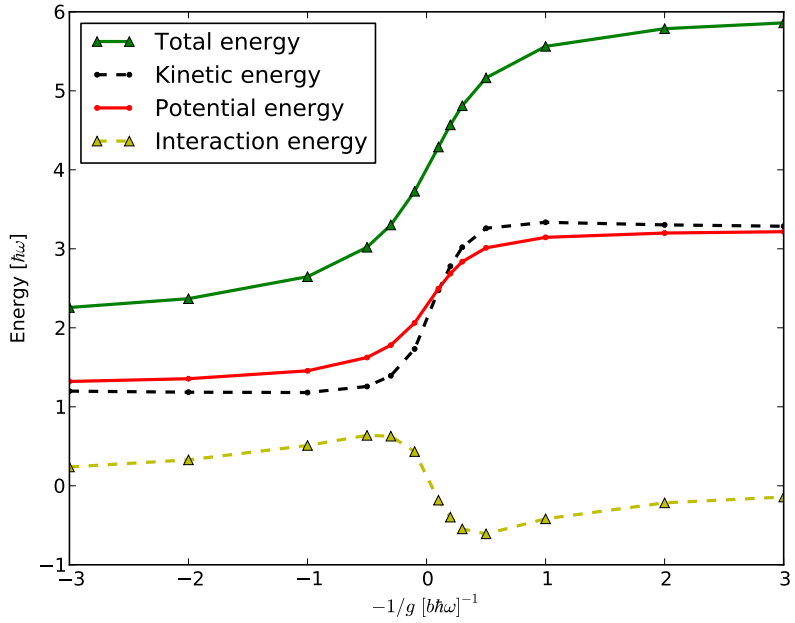

Figure 4.10: Different energy contributions for the lowest odd parity state on the repulsive side in the 2+1 particle system as they evolve through the resonance and into the attractive regime.

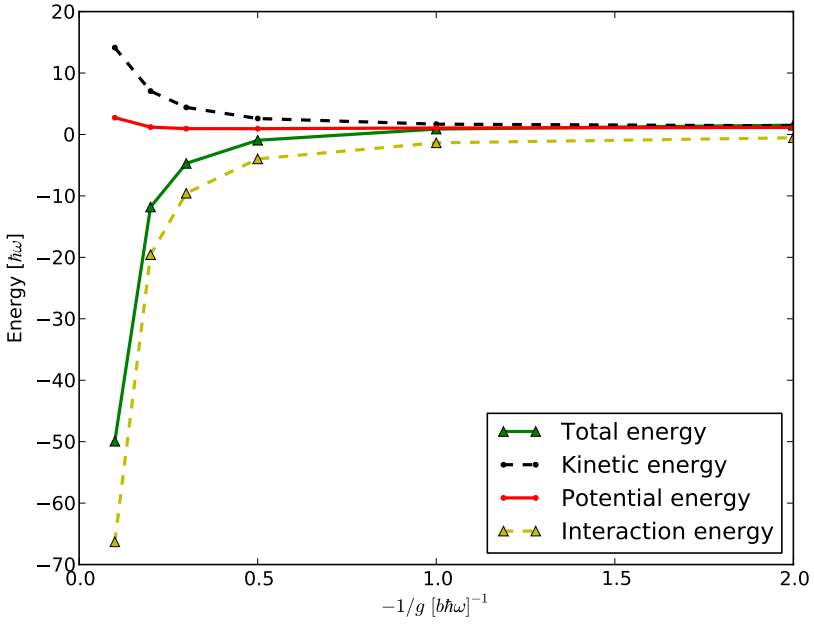

Figure 4.11: Different energy contributions for the lowest odd parity state on the attractive side in the 2+1 particle system as $g \to -\infty$.

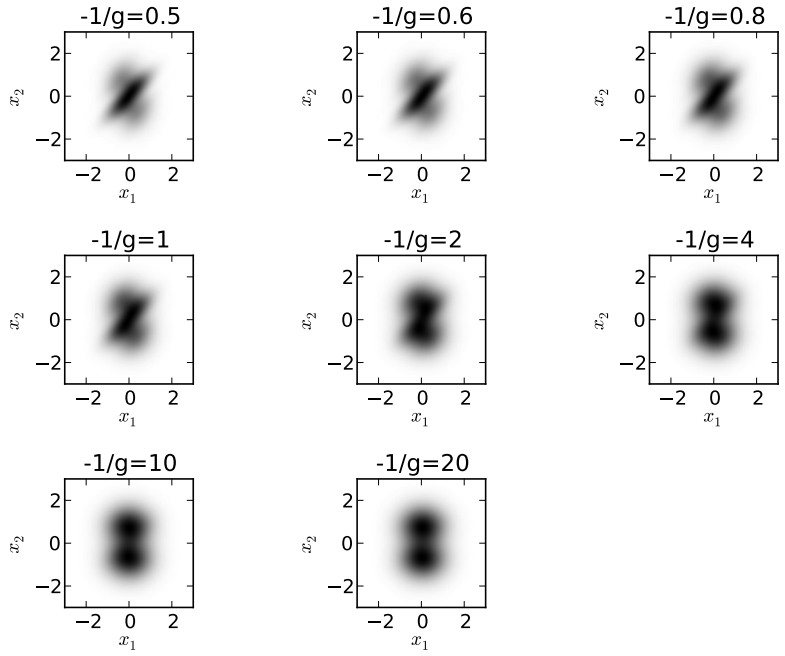

Figure 4.12: Pair correlation function for the lowest odd parity state on the attractive side for $g \to -\infty$ in the 2+1 particle system.

4.3 3+1 system

In Fig. 4.13 the energy spectrum of the 3+1 particle system is shown. This also resembles the Busch model except there are many more states and in particular more states diverging to minus infinity. The higher degeneracy is expected since there are more combinations available with more particles. This makes it very difficult to reach strong attractive interactions by means of numerical methods. The main focus of our discussion will be on the four lowest states on the repulsive side.

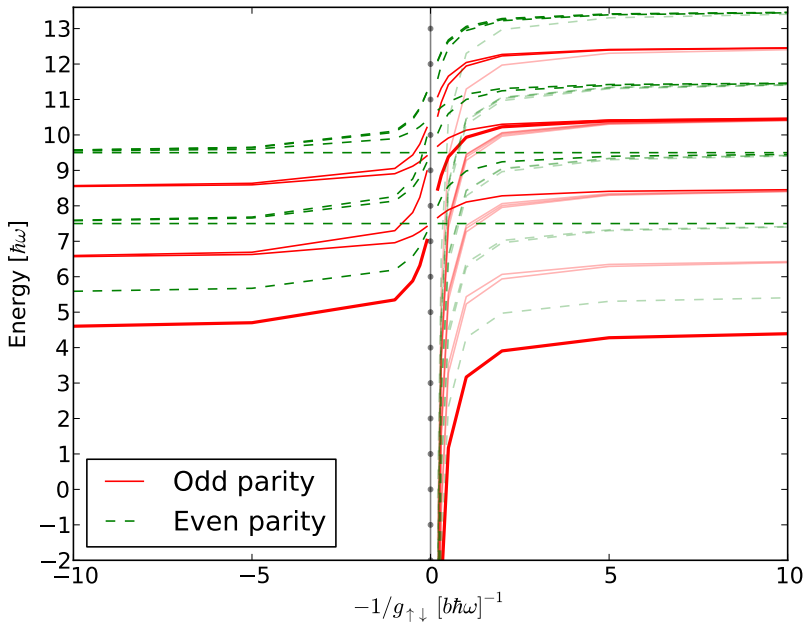

Figure 4.13: Energy spectrum of the 3+1 system.

In Fig. 4.14, Fig. 4.15 and Fig. 4.16 the coordinate space densities of the second lowest odd parity state, lowest odd parity state and lowest even parity state are shown compared to the densities of the second lowest even parity state which is a non-interacting state. We can see, that just as in the 2+1 case, the total coordinate space density approaches the non-interacting states density while the subsystems densities do not.The ground states total density for both parities seems to approach the non-interacting states density slower than the excited odd parity state. This is consistent with Fig. 4.13 where their energy is further away from their limit at $g \to \infty$ since they start out at a lower energy.

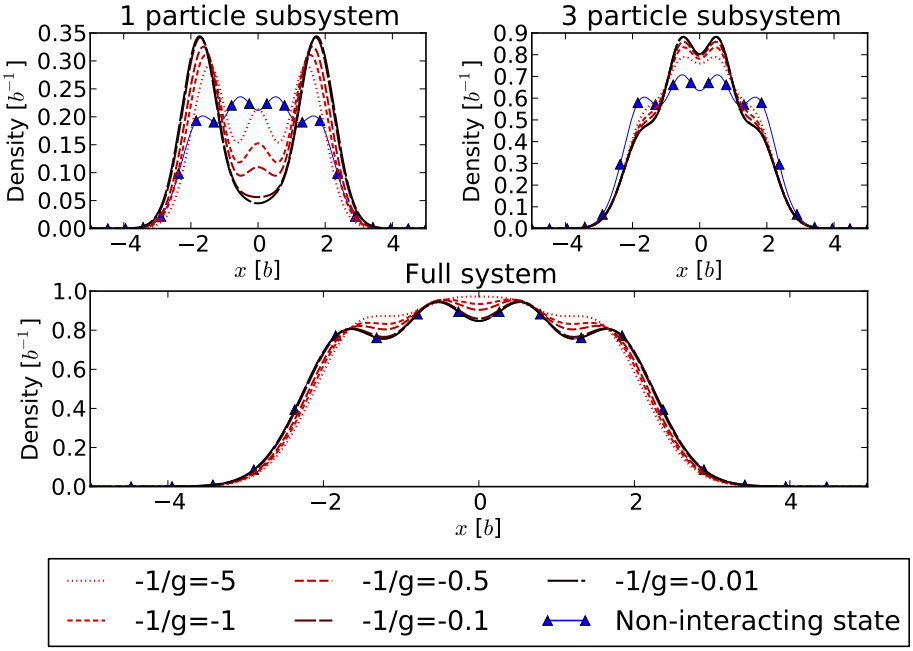

Figure 4.14: Particle coordinate space densities of the second lowest odd parity state of the 3+1 particle system for different interactions. Darker colored curves represent stronger interaction and the blue curve is the density of the second lowest even parity state which is a non-interacting state, i.e. independent of the interaction.

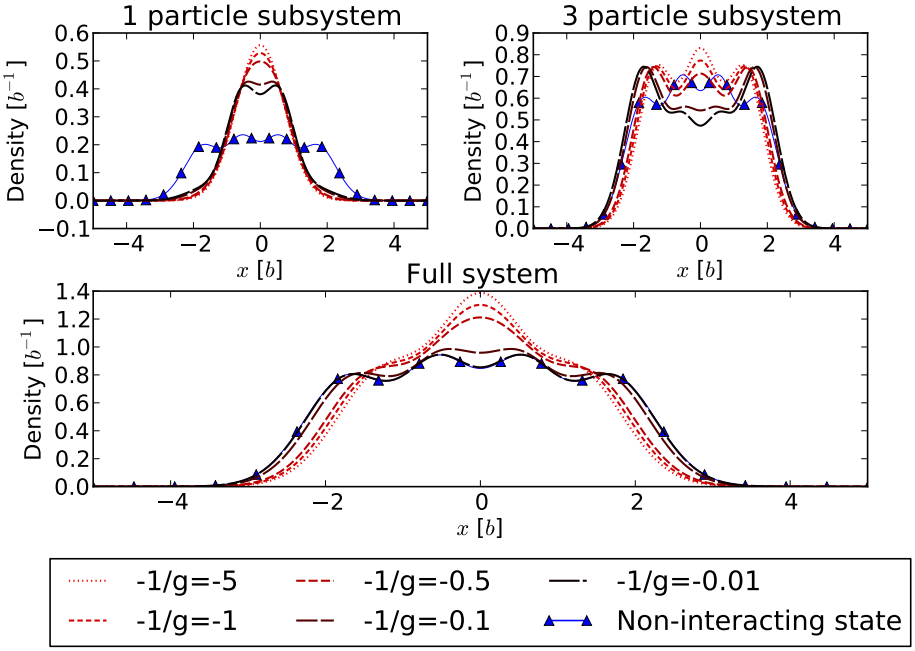

Figure 4.15: Particle coordinate space densities of the lowest odd parity state of the 3+1 particle system for different interactions. Darker colored curves represent stronger interaction and the blue curve is the density of the second lowest even parity state which is a non-interacting state, i.e. independent of the interaction.

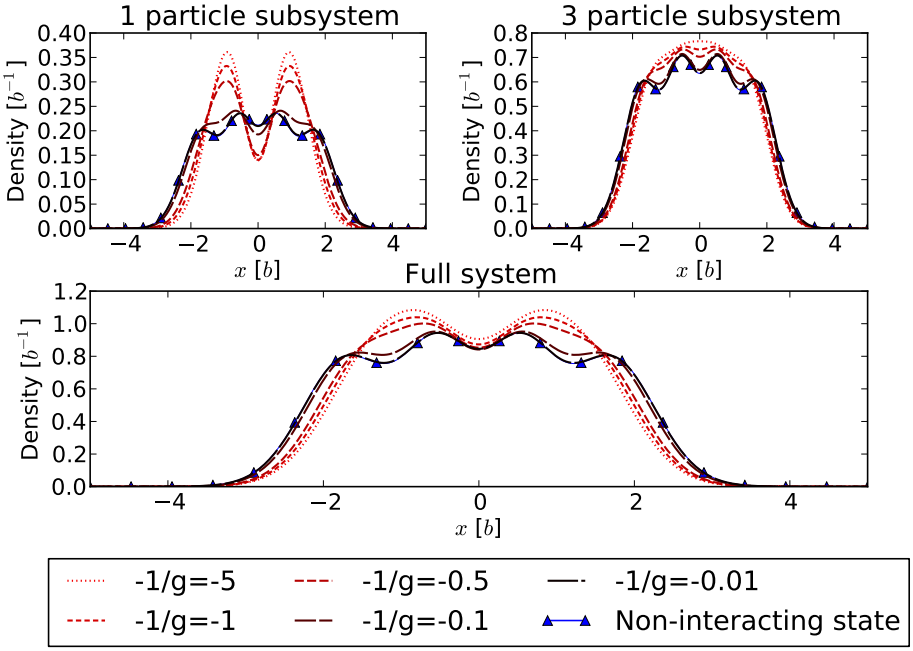

Figure 4.16: Particle coordinate space densities of the lowest even parity state of the 3+1 particle system for different interactions. Darker colored curves represent stronger interaction and the blue curve is the density of the second lowest even parity state which is a non-interacting state, i.e. independent of the interaction.

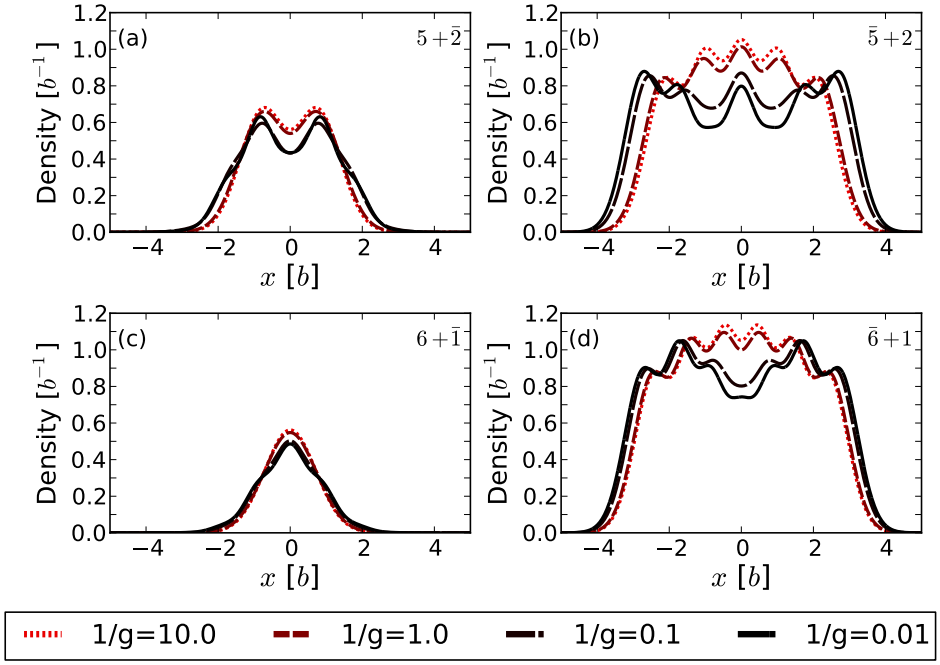

Figure 4.17: Particle coordinate space densities of the ground state for the 5+2 system and the 6+1 system. (a) Density of the two-particle subsystem in the 5+2 system. (b) Density of the five-particle subsystem in the 5+2 system. (c) Density of the one-particle subsystem in the 6+1 system. (a) Density of the six-particle subsystem in the 6+1 system.

Chapter 5

Conclusions and outlook

We have in this project used exact diagonalization to numerically solve a trapped one-dimensional two-component fermionic system for arbitrarily strong contact interaction. The convergence has been speeded up by using an effective interaction which utilizes information from the two-body system to help solve the many particle system. Altough the numerical procedure would in theory work for any interaction and any potential, the available analytical solutions of the two-body system with a contact interaction in a harmonic oscillator potential is a huge advantage. The results of this seemingly unreal quantum mechanical system are of high relevance for experiments on cold atoms where the atoms are trapped in one-dimension effectively realizing this one-dimensional quantum mechanical system. The interactions strength in these experiments can be tuned via a so called Feshbach resonance allowing for very controlled experimental environments that allows for very precise comparison between theory and experiment. The analytical solutions of the two-particle system have already been verified with experiments and in the near future we will hopefully also see the results for the many-particle systems verified in experiments.

The observed convergence rate when using the effective interaction is far superior to the one encountered when using the bare interaction. This makes it possible to reach regimes of strong interaction that are otherwise unreachable, and it is possible to increase the number of particles before being limited by computational power. It is also a huge advantage to have access to the analytical solutions. The convergence of the eigenvalues and eigenvectors with a bare interaction is very bad and just solving the problem numerically in the two-body case requires including a huge amount of basis states. With the analytical solution we get the exact solution for the infinite basis which gives much better convergence in the many-particle case compared to solving the two-body system numerically. Thus if one would study a system with a more realistic external potential, or with a different interaction (including a finite range for example) where no analytic solution exists, it might be a good idea to still try to use the effective interaction generated by the analytic solution and then afterwards try

to correct for the new potential and interaction by e.g. treating the difference with perturbation theory. However, it should be emphasized that the numerical method can be used for an arbitrary interaction and arbitrary potential, altough the convergence might be worse.

There are some interesting features of these systems at fermionization. The phase separation of the spin is one of the more interesting ones. As can be seen in Figs. 4.4 and 4.5 there is a separation in coordinate space of the spin-specific densities. For the odd parity state the single particle has a high probability of being in the center of the potential while the two particles are pushed to the sides, while for the even parity state the opposite happens. The same happens in the 3+1 particle system as shown in Figs. 4.14, 4.15 and 4.16. This can be related to a phenomenon called Stoner ferromagnetism which was described by Edmund Stoner in 1938[14]. This is a theoretical state of a two-component quantum gas where a strong repulsive interaction creates two domains of particles with different spin. The phase separation observed in the few-body systems studied here would thus be a few-body analog to Stoner ferromagnetism. This phase separation also happens for more particles as shown in Fig. 4.17. However, even though Stoner ferromagnetism was predicted in the 1930s, this state of matter has not yet been observed.

This work has been a purely numerical study and a possible continuation would be to try to extract more analytical results. The simple values of the energy values at fermionization suggests that this limit should be completely solvable analytically for an arbitrary number of particles. This is something that is well worth looking into. Which states that connect to each other at fermionization and the structure of the diverging states is also something that might be possible to extract analytically. However, the numerical method discussed here can access all interaction strengths and the fermionization limit is definitely not the only interesting region. For example, there is a maximum in the interaction energy expectation value at intermediate attractive interaction strength as indicated in Fig. 4.10 so this particular region might be interesting to study further.

It might also be interesting to study corrections to the full potential expression as given by Eq. B.1. This potential is not coordinate inversion invariant, so the composition into different parity states is then not possible. The biggest difference however would be the possibility for scattering states since the potential wall on the right side has a finite size. The harmonic oscillator states are all bound states, so a different basis would be needed to be able to include scattering states.

An extension to three dimensions might also be relevant. The asymmetric potential trap used in the experiment in [15] has a ratio between the oscillation frequencies $\omega_\perp/\omega_\parallel \approx 10$ which is actually not that good. When solving for the energy spectrum the cutoff used on the basis states includes states with energy larger than $10\hbar\omega_\parallel$ indicating that one should also start including harmonic os-

cillator states that are excited in the perpendicular direction.

In this thesis we have only considered systems with very few particles, but the excellent convergence suggests that it should be possible to increase the number of particles. The good convergence rate of this method for all values of the interaction strength, and the fact that this method makes it very easy to extract relevant observables like the occupation numbers and particle densities, also allows for very precise comparisons with future experimental results.

Bibliography

[1] M. H. Anderson, J. R. Ensher, M. R. Matthews, C. E. Wieman, and E. A. Cornell. Observation of Bose-Einstein Condensation in a Dilute Atomic Vapor. *Science*, 269(5221):198–201, July 1995.

[2] G. Baym. *Lectures on Quantum Mechanics: Lecture Notes and Supplements in Physics*. Lecture Notes & Supplements in Physics Ser.). Benjamin/Cummings Publishing Company, Advanced Book Program, 1969.

[3] Thomas Busch, Berthold-Georg Englert, Kazimierz Rzażewski, and Martin Wilkens. Two cold atoms in a harmonic trap. *Foundations of Physics*, 28:549–559, 1998.

[4] Cheng Chin, Rudolf Grimm, Paul Julienne, and Eite Tiesinga. Feshbach Resonances in Ultracold Gases. July 2009.

[5] Jane K. Cullum and Ralph A. Willoughby. *Lanczos Algorithms for Large Symmetric Eigenvalue Computations, Vol. 1*. Society for Industrial and Applied Mathematics, Philadelphia, PA, USA, 2002.

[6] M.T. Heath. *Scientific computing: an introductory survey*. McGraw-Hill Higher Education. McGraw-Hill, 2002.

[7] W. Ketterle and N.J. van Druten. Comprehensive review paper on evaporative cooling. *Advances in Atomic, Molecular, and Optical Physics*, 37, 1996.

[8] V S Letokhov, M A Ol'shanii, and Yu B Ovchinnikov. Laser cooling of atoms: a review. *Quantum and Semiclassical Optics: Journal of the European Optical Society Part B*, 7(1), 1995.

[9] P. Navrátil, J. P. Vary, and B. R. Barrett. Large-basis ab initio no-core shell model and its application to $^{12}\mathbf{C}$. *Phys. Rev. C*, 62:054311, Oct 2000.

[10] F. W. J. Olver, D. W. Lozier, R. F. Boisvert, and C. W. Clark, editors. *NIST Handbook of Mathematical Functions*. Cambridge University Press, New York, NY, 2010.

[11] L.P. Pitaevskii and S. Stringari. *Bose-Einstein Condensation*. International Series of Monographs on Physics. Clarendon Press, 2003.

[12] Bateman Manuscript Project, H. Bateman, A. Erdélyi, and United States. Office of Naval Research. *Higher transcendental functions*. Higher Transcendental Functions. McGraw-Hill, 1953.

[13] J. J. Sakurai. *Modern Quantum Mechanics (Revised Edition)*. Addison Wesley, 1 edition, September 1993.

[14] Edmund C. Stoner. Collective electron ferromagnetism. 165, 1938.

[15] G. Zürn, F. Serwane, T. Lompe, A. N. Wenz, M. G. Ries, J. E. Bohn, and S. Jochim. Fermionization of two distinguishable fermions. *Phys. Rev. Lett.*, 108:075303, Feb 2012.

Appendix A

Feshbach resonances

Close to a so called Feshbach resonance it is possible to experimentally alter the interaction strength between atoms by just changing a magnetic field opening up for great control over quantum mechanical systems. The precise mechanisms behind the resonance are quite complicated but we will in this section give some motivation and explain the physics of the resonance. For further reading, and more thorough treatments of Feshbach resonances, see [4].

In scattering theory when dealing with spherically symmetric potentials, one usually decomposes the incoming states in eigenstates of the angular momentum operator. Since the angular momentum operator commutes with the Hamiltonian these different so called partial waves will not interact with each other. Thus we will have a family of different potentials $V_\ell(r)$ corresponding to different partial waves. These come from the matrix elements $\langle \ell, r|V|\ell', r'\rangle = \delta(r-r')\delta_{\ell\ell'}V_\ell(r)$. One calls the subspace with a definite angular momentum ℓ a scattering channel. This is an example of *multi-channel scattering* where the different channels do not mix. Since the different channels do not interact, the result of the scattering event will be just a change in the phase (the phase shift) of the expansion coefficients of the incoming state [13].

Consider, as the simplest example of a Feshbach resonance, a system considering of two different channels with two different potentials. One channel, called the open channel, only has scattering states among the states with positive energy. The other channel, the closed one, has one bound state, see Fig. A.1. The continuum of eigenstates starts at a higher value E_0 than in the open channel. The bound state's energy is denoted E_b which is close to zero.

To describe this system we consider the Hilbert space being made up by two subspaces $\mathcal{A}$ and $\mathcal{B}$ for the open and the closed channel, respectively. The eigenstate can be written as $|\Psi\rangle = |\Psi_A\rangle + |\Psi_B\rangle$. If we let A and B be the projection operators onto the respective subspaces (satisfying $AB = BA = 0$ and $A + B = 1$) we have $|\Psi_A\rangle = A|\Psi\rangle$ and $|\Psi_B\rangle = B|\Psi\rangle$. Consider the time

independent Schrödinger equation

$$H|\Psi\rangle = E|\Psi\rangle \tag{A.1}$$

Here E is approximately equal to the threshold energy for the open channel, since we are considering low-energy scattering. By applying A and B, respectively, we can get two coupled equations

$$\begin{aligned}(E - H_{AA})|\Psi_A\rangle &= H_{AB}|\Psi_B\rangle \\ (E - H_{BB})|\Psi_B\rangle &= H_{BA}|\Psi_A\rangle.\end{aligned} \tag{A.2}$$

where $H_{AB} = AHB$ and $H_{BA} = BHA$ are the off block-diagonal parts of the Hamiltonian and $H_{AA} = AHA$ and $H_{BB} = BHB$ are the parts of the Hamiltonian for the subspaces $\mathcal{A}$ and $\mathcal{B}$, respectively. We can formally solve the second equation $|\Psi_B\rangle = \frac{1}{E-H_{BB}} H_{BA}|\Psi_A\rangle$ and then substituting this into the first yields

$$(E - H_{\text{eff}})|\Psi_A\rangle = 0 \tag{A.3}$$

where $H_{\text{eff}} = H_{AA} + H_{AB}\frac{1}{E-H_{BB}}H_{BA}$.

We can expand the operator $\frac{1}{E-H_{BB}}$ in eigenstates of the closed channel Hamiltonian H_{BB}

$$\frac{1}{E - H_{BB}} = \frac{1}{E - E_b}|E_b\rangle\langle E_b| + \int_0^\infty \frac{1}{E - E(\lambda)}|\phi_\lambda\rangle\langle\phi_\lambda| \tag{A.4}$$

where the integral is over all continuous states. Close to the resonance (when $E_b \approx E$) the term from the bound state diverges and thus we can neglect the contributions from the continuous states.

$$\frac{1}{E - H_{BB}} \approx \frac{1}{E - E_b}|E_b\rangle\langle E_b| \tag{A.5}$$

The open channel Hamiltonian is given in relative coordinates by

$$\langle x|H_{AA}|x'\rangle = \delta(x - x')\frac{\nabla^2_{x'}}{2m} + \delta(x - x')V_{\text{open}}(|x - x'|) \tag{A.6}$$

and now we see that the effective Hamiltonian will be

$$\langle x|H_{\text{eff}}|x'\rangle = \delta(x - x')\frac{\nabla^2_{x'}}{2m} + \delta(x - x')V_{\text{open}}(|x - x'|) + \frac{\langle x|H_{AB}|E_b\rangle\langle E_b|H_{BA}|x\rangle}{E - E_b} \tag{A.7}$$

In the experimental systems, the different channels correspond to different hyperfine states of the atoms. The difference in magnetic moments makes it possible to change the energy spectrum of the closed channel with an external magnetic field (and in particular the energy of the bound state). By the Zeeman effect this change is $\Delta\mu B$ where B is the magnetic field strength and $\Delta\mu$ is the difference in magnetic moments. Thus close to the resonance we have

$E - E_b = \Delta\mu(B_0 - B)$, where we defined $B_0 \equiv \frac{E}{\Delta\mu}$.

Assuming that the extra term in the Hamiltonian is a local interaction, namely that $\langle x|H_{AB}|E_b\rangle \propto \delta(x)$, this extra term has the form of a delta function interaction

$$\frac{\langle x|H_{AB}|E_b\rangle\langle E_b|H_{BA}|x'\rangle}{E - E_b} = g\delta(x - x')\delta(x) \tag{A.8}$$

This can also be motivated by examining the scattering length of the system[4]. Close to the resonance this term will dominate and thus the whole system can be modelled with a delta function interaction, where the interaction strength is $g \propto \frac{1}{B_0 - B}$. In particular, the interaction strength goes to $\pm\infty$ at the resonance, see Fig. A.2.

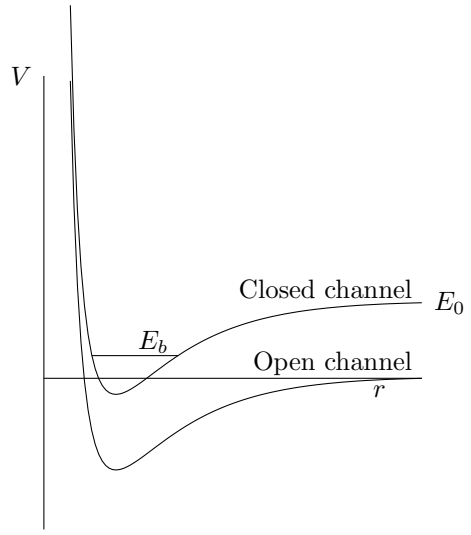

Figure A.1: Illustration of the potentials of the different channels. E_b denotes the energy of the bound state and E_0 is the threshold energy of the continuum spectrum for the closed channel.

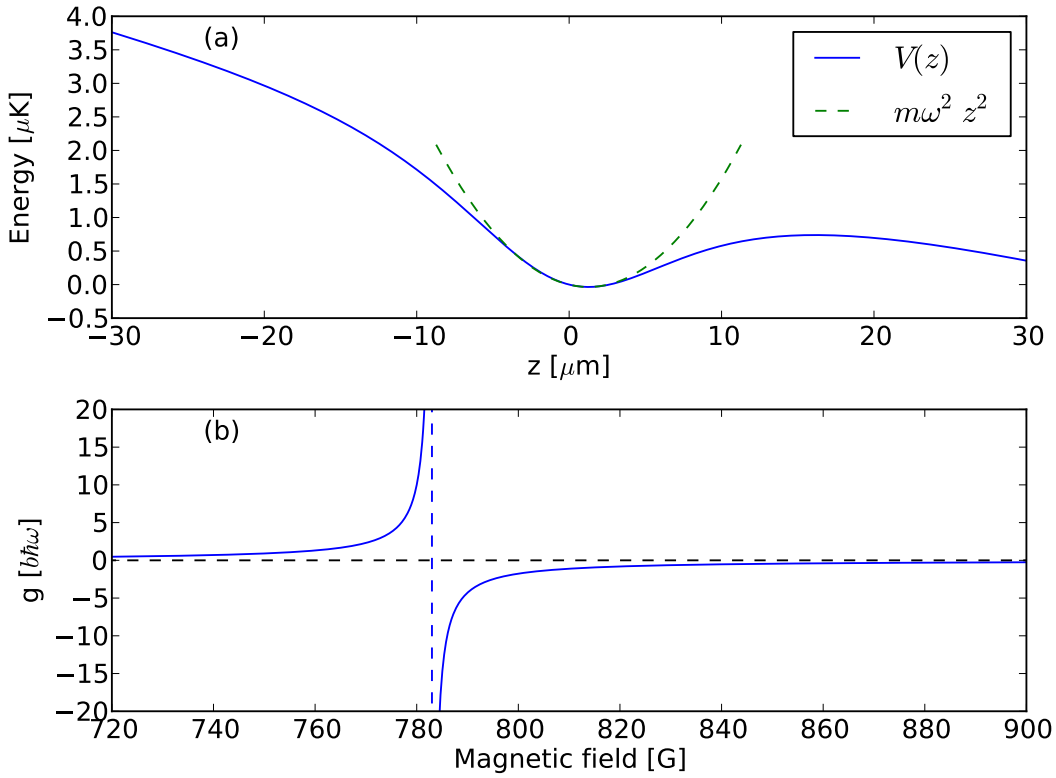

Figure A.2: (a) The real potential and the harmonic oscillator approximation. (b) The coupling coefficients as a function of the magnetic field. Parameters are taken from [15].

Appendix B

Trapping potential

In the most relevant experiments[15] the trapping potential is created by a tightly focused laser beam and a magnetic field gradient. In one dimension it has the form[15]

$$V(z) = V_0(1 - \frac{1}{1 + (z/z_r)^2}) - \mu_m B z \tag{B.1}$$

where B is the magnetic field strength, z_r is the Rayleigh range of the laser beam and μ_m is the magnetic moment of the atoms. The potential is shown in Fig. A.2. In this thesis we will only consider bound states trapped at the minimum of this potential. Therefore, we will approximate the trap as a harmonic oscillator potential. Because of the linear magnetic field term, this potential is not inversion invariant, thus parity is not a good quantum number (but will be in the harmonic oscillator approximation). The linear term also shifts the minimum of the potential well. To get some insight into the behaviour of the harmonic oscillator we will derive the oscillator frequency expressed in the parameters of the original potential. Let us define $\mu_m B z_r = C$ and work in units of z_r, so the potential looks like

$$V(z) = V_0(1 - \frac{1}{1 + z^2}) - Cz \tag{B.2}$$

The derivative is

$$V'(z) = V_0 \frac{2z}{(1 + z^2)^2} - C. \tag{B.3}$$

For small $z \approx 0$ we have $1 + z^2 \approx 1$ yielding $z_0' = \frac{C}{2V_0}$ as our first approximation to the minimum of the potential. Let z_0 be the real minimum. To get the oscillator frequency we take the second derivative

$$V''(z) = \frac{2V_0}{(1 + z^2)^2} - \frac{8V_0 z^2}{(1 + z^2)^3} \tag{B.4}$$

Using that $V_0 \frac{2z_0}{(1+z_0^2)^2} - C = 0$ we obtain

$$m\omega^2 = V''(z_0) = \frac{C}{z_0} - C\sqrt{8Az_0C} \tag{B.5}$$

If we now use $z_0 \approx z_0'$ we obtain the expression

$$m\omega^2 = 2V_0 - 2C^2 \tag{B.6}$$

Going back to the original parameters we have

$$m\omega^2 = \frac{2V_0}{z_r^2} - 2\mu_m^2 B^2 \tag{B.7}$$

In the whole project we have assumed that we just have a harmonic oscillator potential $V(x) = m\omega^2 \frac{x^2}{2}$.